February 2014

Ph.D. Dissertation

Development of β-amyloid purification method and its identification as an inducer of nuclear scaffold protease-mediated lamin cleavage which occurs independently of caspase activation

Graduate School of Chosun University

Department of Bio-Materials

Vijaysankar Ramasamy

Development of β-amyloid purification method and its identification as an inducer of nuclear scaffold protease-mediated lamin cleavage which occurs independently of caspase activation

β-아밀로이드 정제방법 개발과 nuclear scaffold

단백질분해효소의 활성화에 의한 lamin 의

절단에 관한 연구

24th February 2014

Graduate School of Chosun University

Department of Bio-Materials

Vijaysankar Ramasamy

Development of β-amyloid purification method and its identification as an inducer of nuclear scaffold protease-mediated lamin cleavage which occurs independently of caspase activation

Advisor: Prof. Il-Seon Park

This dissertation is submitted to the Graduate School of Chosun University in partial fulfillment of the requirements for the degree of Doctor of Philosophy in Science

October 2013

Graduate School of Chosun University

Department of Bio-Materials

Vijaysankar Ramasamy

This is to certify that the Ph.D. dissertation of Vijaysankar Ramasamy has successfully met the dissertation requirements of Chosun University.

Chairman:Prof. Song Yub Shin .....

Member: Prof. Il-Seon Park .....

Member: Prof.Takbum Ohn .....

Member: Prof. Jung Hee Lee .....

Member: Prof. Kun Ho Lee .....

December 2013

Graduate School of Chosun University

CONTENTS

LIST OF FIGURES

Abstract

Development of β-amyloid purification method and its identification as an inducer of nuclear scaffold protease-mediated lamin cleavage which occurs independently of caspase activation

Vijaysankar Ramasamy
Advisor: Prof. Il Seon Park
Department of Biomaterials
Graduate School of Chosun University

The aggregation and accumulation of Aβ plays a significant role in the pathogenesis of Alzheimer's disease. Aβ oligomeric aggregates are believed to be the main toxic species underlying the pathogenicity. Understanding the mechanistic details of Aβ-induced cell death is crucial to developing effective strategies to prevent and control AD. As

evidenced by a number of cell-based experiments and animal model studies, there are good correlations between the pathogenesis and structural species of Aβ. In this study, an efficient system was constructed to purify the peptides in soluble form. The target peptides were expressed as inclusion bodies. Aβs were purified after solubilization of fusion protein in urea and cleavage by a deubiquilinating enzyme. The cleaved peptide solution were then subjected to Ni-NTA column and Reverse phase–HPLC chromatography to obtain homogeneous Aβ peptide. Further, to study the Aβ binding or interacting proteins, a FLAG tagged Ab42 vector system was developed. The fusion protein was overexpressed, purified and their binding efficiency was analyzed by using Immunoprecipitation and confocal imaging methods.

. Next, we made an attempt to correlate specific protease(s) to selected cell death-inducing agent. Particularly, non-caspase proteases functioning in the cell death were interested, because roles of the enzymes in the death process are relatively less understood. β-amyloid (Aβ), a hallmark peptide of Alzheimer's disease (AD), was chosen as a death inducer, because it is important in pathogenesis of the disease, and its cell death inducing mechanism is not well understood.

Cytotoxicity, Caspases and their substrates processing were analyzed using immunoblotting and enzyme assays. Our results show that lamin A and B reduction and consequent nuclear morphological change occur in cells treated by Aβ42 before caspase activation. Data of our study indicate that the reduction of lamin proteins may be due to NS protease function. Suppression of NS protease by its inhibitor, AAPF-CMK, effectively inhibited the cell death induced by Aβ42.This study provides an idea that inhibition of NS protease might be an effective way to control pathological process of AD.

요약

β-아밀로이드 정제방법 개발과 nuclear scaffold 단백질분해효소의 활성화에 의한 lamin의 절단에 관한 연구

Aβ의 응집과 축적은 알쯔하이머병의 중요한 병인이다. 여러 구조체 중 Aβ oligomer가 가장 세포독성이 강하다. 이 세포독성의 기전을 이해하기 위해서는 다량의 Aβ의 준비가 필요하다. 또한 여러 변이체가 필요한데 그 중 flag등에 의해 tag된 Aβ등은 Aβ에 결합하는 단백질의 확인등에 매우 유용할 것이다. 따라서 본 연구에서는 이 펩티드를 정제하기 위한 방법을 고안하였다. 이 펩티드는 inclusion body의 형태로 발현시켜 urea에 녹인 fusion 단백질 상태로 준비하고 이어 deubiquilinating enzyme으로 절단시켰다. fusion 단백질로부터 절단된 Aβ를 Ni-NTA column과 reverse phase-HPLC chromatography로 순수한 Aβ를 얻었다. 이를 이용하여 Aβ의 세포독성을 연구하였다. HeLa 세포에 Aβ oligomer를 처리하고 그 독성과 apoptosis의 중요효소인 caspase 활성화, 그 기질의 processing을 immunoblotting과 enzyme 활성조사를 통해 분석하였다. 오랫

동안 세포에 Aβ를 처리하면 농도 의존적으로 caspase 활성과 그 기질의 processing이 증가하였다. 그러나 짧은 시간을 처리하면 그렇지 않았다. 그러나 세포독성은 이 짧은 시간에 관찰되었는데 이는 Suc-AAPF-CMK에 의해 저해가 되어 이 세포독성이 caspase와는 상관없이 일어나며 아마도 nuclear serine protease와 연관있으리라 생각되었다. 이 연관성은 이 효소의 기질인 lamin A와 B가 절단되는 것으로 확인되었으며 confocal imaging등의 후속 실험에 의해 재차 확인되었다. 이는 Aβ가 caspase활성화와 상관없이 nuclear scaffold protease의 활성화에 의해 그 세포독성을 나타냄을 의미한다.

I.INTRODUCTION

I.1 Amyloid beta cascade hypothesis

Accumulation of amyloid beta (Aβ) as amyloid plaques in the patient's brain is the primary event in the pathogenesis of Alzheimer's disease (AD). Other neuropathological changes such as neurofibrillary tangles (NFTs), synaptic degeneration and neuronal cell loss are secondary and appear as a consequence of Aβ deposition. Aβ is a 4.5 KDa peptide consist of 39-42 amino acid residues [1-5]. It is a proteolytic fragment cleaved from the amyloid beta precursor protein (APP) by two proteases, β- and γ- secretase. A third secretase, α- secretase cleaves the Aβ sequence itself and is therefore usually considered as nonamyloidogenic. α- secretase (a member of the ADAM family of metalloprotease) and β- secretase (a membrane bound aspartyl protease also called BACE) cleave the ectodomain of APP, resulting in the shedding of APPsα- and APPsβ. γ- secretase finally cleaves the transmembrane domain of the APP carboxy terminal fragments (α-CTF and β-CTF), releasing p3 and Aβ peptide [6,7]. Aβ42 is neurotoxic and more hydrophobic than Aβ40, thus it has stronger tendency to

oligomerize and aggregate. These neuronally generated Aβ monomers and perhaps various oligomers are presumed to equilibrate within the interstitial fluid of the brain. The imbalance between Aβ production and Aβ clearance is the basis for the formation of amyloid plaques. Both extracellular and intracellular accumulation of Aβ initiates a cascade of events leading to the Neurodegeneration: synaptic and neuritic injury, oxidative damages, microglial and astrocytic activation, altered neuronal ionic homeostasis, activation of Caspases / proteases and finally cell death [7-11].

I.2 Amyloid beta aggregation and toxicity

Several pathogenic Aβ species that precede plaque formation have been isolated from AD brains. These include low molecular weight (LMW) oligomers; Aβ derived diffusible ligands or high molecular weight (HMW) oligomers, protofibrils and fibrils. Aβ42 aggregation is a complex multi-step reaction; the exact mechanism of aggregation is not fully understood [12, 13]. A general view of the aggregation of soluble monomers into insoluble fibrils involves two steps (i) nucleation, the formation of the nucleus by association of a series of monomeric

peptides, (ii) and extension, the subsequent addition of monomers to the existing nucleus. Aβ40 and Aβ42 have been shown to have distinct aggregation pathways at early stage. Initial aggregation of Aβ42 involves the formation of pentamers/ hexamers units, referred to as Paranuclei [9, 12]. Then Aβ42 paranuclei further oligomerize to larger forms, i.e. large oligomers, protofibrils and fibrils. Two additional hydrophobic residues Ile at position 41 and Ala at position 42 may play important role in enhanced toxicity and faster aggregation properties of Aβ42 compared to Aβ40 [14 – 16].

Previous reports implicated that the deposited fibrils around the neuronal cells are responsible for the cell death in AD brains. But recent evidences suggest that this toxicity may be linked to the oligomers rather than the insoluble fibrils. While both are found in the brains of AD patients, soluble Aβ oligomers are better correlated with the disease severity than the fibrillar deposits. Furthermore oligomers are found both extracellularly and intracellularly and are capable of moving between the extracellular space. However Aβ oligomer structure, size, conformation and interrelationship with other amyloid aggregates, as well as the exact mechanism of oligomer induced toxicity remains elusive [17- 20].

I.3 Amyloid beta: Interaction with membranes and intracellular proteins

The mechanisms through which of Aβ monomers, oligomers and other APP metabolites that lead to synaptic damage and neurodegeneration is not completely clear. A number of possibilities are under investigation, one of the main focuses is receptor mediated toxicity. Several research groups reported that extracellular Aβ oligomers binds the cell surface leading to functional disruption of number of receptors including the N-methyl-D-aspartate (NMDA) receptor(1), Nerve growth factor (NGF) receptor, p75 neurotropin (p75NTR) receptor. Aβ disrupts NMDAR dependent long term potentiation by interfering with Calcinurin and Calmodulin dependent protein kinase II. Another study showed that Aβ oligomers bind to the Frizzled receptors and inhibit the Wnt signaling pathway which is essential for axon guidance and synapse formation. A recent study identifies the cellular prion protein (PrP^C) as an Aβ oligomer receptor [21 – 26]. The maintenance of plasma membrane integrity is critical for cell viability. An increase in membrane permeability and intracellular calcium concentration has long been associated with amyloid pathogenesis.

Recent reports also proved that Aβ can form membrane channels and disrupt calcium homeostasis. A study by Demuro et al showed that amyloid oligomers consistently produce rapid and dramatic elevations in Ca^{2+}, whereas equivalent concentrations of monomers or fibrils do not. Once Aβ channels are formed on neuronal membranes, the disruption of calcium and other ion homeostasis may promote numerous degenerative processes, including free radical formation, and phosphorylation of tau, alterations in glutamate receptors and excitotoxicity; circuitry hyper excitability; mitochondrial dysfunction [27 – 33]; lysosomal failure and alterations in signaling pathways related to synaptic plasticity and neurogenesis.

In addition to extracellular Aβ, there is a large body of evidence to demonstrate that Aβ accumulates intracellularly. Several pathways have been proposed to mediate the event. Internalization via endocytosis and accumulation in the endosomal / lysosomal system have been suggested by an earlier study. It has been reported that Aβ is internalized through the advanced glycation end products receptor (RAGE). Another data provided evidence that Aβ accumulation in neurons inhibits the activities of proteasome and deubiquitylating enzymes. Accumulation of Aβ has also been observed in mitochondria

[30-36]. Progressive accumulation of intracellular Aβ in mitochondria is related to diminished enzymatic activity of respiratory chain complexes III and IV, and a reduced rate of oxygen consumption. The interaction of Aβ with amyloid beta binding alcohol dehydrogenase (ABAD) leads to the dysfunction of mitochondria and generation of reactive oxygen species (ROS) by abrogating ABAD's 4-HNE detoxifying properties. Binding of Aβ to the α7 nicotinic acetylcholine receptor with high affinity results in receptor internalization and accumulation of Aβ intracellularly.

Several studies have shown that a number of signaling proteins, including fyn kinase [37], glycogen synthase kinase-3β [GSK3β] and cyclin-dependent kinase-5 [CDK5], are involved in neurodegenerative progression of AD. Other signaling pathways that have been investigated include members of the MAPK family such as ERK and JNK as well as other pathways such as p21-activated kinase. Abnormal activation of signaling pathways might lead to synaptic failure and altered neurogenesis by promoting Tau phosphorylation and aggregation, cytoskeletal abnormalities, activating Pro-apoptotic pathways and induces calcium and calpain dependent proteolysis [37-43].

Caspases and Caspase-independent mechanisms in apoptosis

Caspase is one of well-known proteases related to cell death [44]. The apoptotic enzyme is synthesized as a zymogen form which is activated by apoptotic signal. Among the two well-defined apoptotic pathways, receptor-mediated apoptosis, or extrinsic apoptosis is characterized by the formation of the death-inducing signaling complex (DISC). On the other hand, chemical-induced apoptosis or caspase-dependent intrinsic apoptosis leads to mitochondrial damage, resulting in the release of cytochrome c which associates with caspase-9, dATP and an adaptor protein Apaf-1 to form a multiprotein complex called apoptosome. The DISC and apoptosome complex activate procaspase-8 and procaspase-9, respectively. Once activated, caspase-8 and -9 then process effector caspases, including caspase-3, -6 and -7 which are responsible for most of the cleavage events observed during apoptosis. Beside the two apoptotic pathways, endoplasmic reticulum stress involved in neurodegenerative disease including Alzheimer's disease induces caspase-4 activation by the unfolded protein response signaling pathway [45].

Other proteases than caspases have been identified to participate in the death process. For example, a mitochondrial serine protease Omi/HtrA2 is released in the cytosol, where it contributes to apoptosis through both caspase-dependent and -independent pathways [46]. It proteolytically removes not only natural inhibitors of caspase such as XIAP and cIAP1 to assist caspase activation, but also many other target proteins which might mediate caspase-independent apoptosis. Lysosomal cathepsin proteases are other example for death-inducing protease. They are released to cytosol by a process known as lysosomal membrane permeabilization [48]. The proteases in cytosol can induce both caspase-dependent and –independent cell death (reviewed jmcb 5:214). The calcium-dependent proteases, calpains, have been also implicated in cellular apoptotic processes (47). The proteases process several members of the Bcl-2 family of cell death regulators and caspases [49]. The ubiquitin-proteasome system also contributes to cell death (50). Besides those exemplified proteases, other proteases such as matrix metalloprotease, amino peptidase and have been suggested to play a critical role in apoptosis or other cell types of cell death [51].

I.4 Amyloid beta and Apoptosis

The eventual consequence of Aβ interactions to extra- and intracellular proteins is the induction of cell death process through different biochemical events such as the activation of caspases, which has been a strong evidence for involvement of apoptosis in the death process. Extensive evidence shows that apoptosis is involved in neuronal loss in AD [52]. The apoptosis, also known as programmed cell death, involves a series of biochemical events, both mitochondrial and non-mitochondrial. The mitochondria-mediated apoptosis is characterized by the formation of apoptosome, a multiprotein complex composed of cytochrome c released from mitochondria, Apaf-1, dATP and Caspase-9 which becomes activated in the complex [53]. On the other hand, extracellular ligands such as TNFα, CD95 and TRAIL bind to the death receptors to form death inducing signaling complex (DISC) which activate caspase-8 in non-mitochondrial receptor mediated apoptosis [54]. Once apoptosome complex and DISC activate the initiator caspases, procaspase-9 and procaspase-8 respectively, it process the effector caspases such as caspase-3, -6 and -7 which are responsible for most of the downstream effects of apoptotic processes. Studies have shown that Aβ induced the apoptosis process both *in vitro*

and *in vivo* systems. Several hypotheses have been proposed for the mechanisms followed by Aβ to induce apoptosis. The mitochondrial release of apoptosis inducing factor (AIF) in cultured neurons ( ) and the release of cytochrome c from isolated mitochondria [53] in presence of Aβ have been suggested, which subsequently initiates a caspase-independent apoptosis by causing DNA fragmentation and chromatin condensation [55]. On the other hand, direct induction of apoptosis by Aβ has been reported by demonstrating the activation and processing of caspase-3 in rat cortical neurons after Aβ application. The presence of caspase inhibitor has been found to block Aβ induced apoptosis without affecting the cell death by the peptide, which indicates different pathways following by Aβ to kill the cells. The exact mechanism of Aβ induced apoptosis and its correlation with cell death, however remains indistinct.

I-6. Outline of the Thesis:

The thesis focused on development of β-amyloid purification method and tried to understand the role of amyloid beta in caspase processing and cytotoxicity. The initial part of the thesis focused on the development and comparison of two methods of β-amyloid purification

and its positivities. The later portion investigates the role of β-amyloid as an inducer of nuclear scaffold protease that cleaves nuclear lamin proteins independently of caspases activation.

1. An improved method was discussed for the production of recombinant amyloid beta peptide by comparing two different methodologies. Amyloid beta co-expressed with inclusion body forming or Solubilization facilitating fusion partners were used for the study.

2. To explore and understand the amyloid beta interacting proteins a FLAG tagged Aβ system was developed, purified and its efficiency was analyzed.

3. A comprehensive study has been carried out to better understand the Aβ mediated caspase processing and early events of cytotoxicity. Protease inhibitor Screening (PIS) method was applied to identify the inhibitors that can reduce the cell death induced by Aβ42. The results provides an interesting clue towards a Nuclear Scaffold protease and its lamin cleaving property independently caspase activation.

4. In addition, experiments were carried out to understand the interaction and effect of Aβ42 on purified recombinant Caspases and also in cultured cells.

II. Purification of recombinant β-amyloid peptide expressed with inclusion body-forming or solubilization-facilitating fusion partner proteins

II-1. INTRODUCTION

The proteolytic cleavage of the amyloid precursor protein by α-, β- and γ- secretases generates 36-43 amino acid-long β-amyloid (Aβ) [1-4]. The native Aβ forms β-sheet-rich intermediate structures after the spontaneous conformational changes. The intermediate peptides are structurally unstable in the aqueous environment and interact with each other to form aggregates such as oligomers, protofibrils and fibrils [5-7]. Those aggregates play a critical role in determination of cell fate. It was suggested that the progressive deposition of the aggregated Aβ peptides in brain parenchyma and cerebral blood vessels leads to the neurodegenerative disorder, Alzheimer's disease (AD) [8]. Recent studies, however, support soluble Aβ42 oligomers and protofibrils formed during Aβ fibrillogenesis as a principle inducer of the neuronal cell death and the disease, because they are more toxic than the monomeric species and fibrils and there are evidences of correlation of the soluble peptides and AD pathogenesis [5, 7].

Understanding the mechanistic details of Aβ-induced cell death

is crucial to developing effective strategies to prevent and control AD. As evidenced by a number of cell-based experiments and animal model studies, there are good correlations between the pathogenesis and structural species of Aβ. For those studies, Aβ peptide and its natural variants such as those associated with familial AD (FAD) have been widely used and various methods have been employed to prepare the peptide. Chemical synthesis of the peptide has been a conventional method for preparation of Aβ peptide. However, the high contents of hydrophobic amino acid and relatively large size of the peptide make the synthesis difficult [56, 57. 58]. Restrictions often encountered in the chemical synthesis of such peptides are on-resin aggregation resulting in inferior yields, chemical and physical heterogeneity and impurities (59). To circumvent many of those problems, recombinant technology has been developed, in which Aβ peptide is expressed in E. coli and is purified by conventional purification methods [60]. Using the methods with additional site-directed mutagenesis, desired Aβ sequence and length variants could be readily prepared. The method was also applicable to preparation of other amyloid-forming peptides. The purified recombinant Aβ42 (42 amino acid-long Aβ) showed faster aggregation and slightly higher toxicity compared with synthetic Aβ42 [61]. The

robust amyloidogenic property and toxicity of the recombinant Aβ42 was speculated to be due to the absence of impurities found in synthetic Aβ which may prevent or slow Aβ incorporation into growing Aβ fibrils [61]. However, biological production of Aβ peptide is not easy task, either, because of its propensity of aggregation, resulting in difficulty in the following purification process.

II-2. Previous results

Recombinant Aβ peptide could be expressed alone without other partner proteins [ref]. However, additional methionine was present in the N-terminal end of the peptide and removal of the amino acid greatly reduced the productivity of the method. On the other hand, methods employing a fusion protein composed of Aβ and partner proteins facilitating the expression and purification steps were shown to be efficient in generation of pure, authentic Aβ peptide. Thus, we here focused on Aβ fusion proteins in the current protocol. As a fusion partner, several proteins such as maltose binding protein [62, 63, 64] [65, 66], ubiquitin and NANP have been previously employed. A cleavage site is also included in the fusion proteins to cleave off the partner protein from the target Aβ peptide.

Most of fusion proteins constructed and utilized for purification of Aβ peptide generally formed inclusion bodies except MBP-based construct [60]. The inclusion bodies containing Aβ fusion protein was solubilized by chaotrophic agents such as urea and guanidine for the following cleavage reaction and purification steps. We have been concerned with two points in the overall steps of the purification: i) the chaotrophic agents could interfere with the cleavage reaction which, usually mediated by enzymes, was undertaken after the solution of the fusion protein was diluted with buffers in the several studies (ref). In the case, the fusion protein might aggregate again to reduce the performance of the cleavage reaction; ii) after the cleavage, Aβ might start the fibrillogenic process, generating several heterogeneous structural species of the peptide. Fibrils and other aggregates of Aβ peptide might result in problems in the next step of purification.

Usp2-cc, a deubiquitylating enzyme, retains its activity even in the presence of 3-4 M urea (ref). This implies that the cleaving step can be performed without removal of urea and moreover, the chemical prevents aggregation of cleaved peptide [60], enabling us to carry out the whole purification steps without removal or dilution of urea. A His_6-GroES-ubiquitin-Aβ fusion protein was constructed to purify Aβ by

exploiting the findings: His_6 was for the affinity purification of the fusion protein; a bacterial chaperon protein GroES was selected as a fusion partner because the fusion protein was relatively small (10.4~kDa), highly expressed in E. coli and formed the inclusion bodies [60]; ubiquitin was for the cleavage.

His_6-GroES-ubiquitin-Aβ fusion protein was highly expressed in E. coli and major parts of the protein were recovered as inclusion bodies (200 mg/1 liter culture). The fusion protein comprises the main part of inclusion bodies (approximately 80%), which facilitated the next step of purification. The inclusion bodies were initially solubilized in a buffer containing 6 M urea and then diluted with the same buffer to make the final concentration of urea 3 M under which the fusion protein was still soluble and the cleaving enzyme Usp2-cc was active enough to cleave off Aβ peptide, as expected. The Aβ peptide maintained its soluble state even after the cleavage, which enabled us to apply the reaction mixture directly to a reverse phase column. ~8~15 mg peptide was obtained per 1 liter culture of the bacteria depending on Aβ variants.

The following development to purify Aβ peptide was focused on construction of a fusion protein that is soluble without the aid of the chaotrophic agents. This system would be efficient in purification of

aggregation-prone proteins and peptides, because it could enable purification of those proteins and peptides in soluble form without the solubilization steps (ref). This made solubilization and refolding process unnecessary for recovery of biological activity of the proteins and peptides. The MBP-Aβ fusion protein was a potential system for the purpose, because the MBP-TEV protease recognition site-Aβ40 fusion protein was expressed as a soluble protein and the target peptide 40 amino acid-long Aβ40 was readily purified from the protein by cleavage by TEV protease and several steps of chromatography. MBP-$(Ala)_5$-Aβ42 was also recovered in the soluble part of E. coli cell extract, although authentic Aβ peptide was not purified (ref). However, Aβ42 has not been purified from the soluble part of E. coli cell extract to our knowledge in the system. Furthermore, our previous trial to employ the MBP system showed that large part of MBP-Aβ fusion proteins were recovered in the inclusion bodies [60]. We therefore searched for other protein as a fusion partner that can make whole fusion protein soluble. After screening *E. coli* proteins, we selected trigger factor protein (TF) as a fusion partner for producing the soluble fusion protein without aid of chaotropic agents [60]. Ubiquitin was also inserted between TF and Aβ for the cleavage of fusion partner as the GroES system. His_6-TF-

ubiquitin-Aβ protein was soluble and ready for the next cleavage and purification steps without any aid of chaotrophic agents, complying with the wanted property. Comparable amount (~8 mg of Aβ42 peptide per 1 liter of E. coli cell culture) was produced.

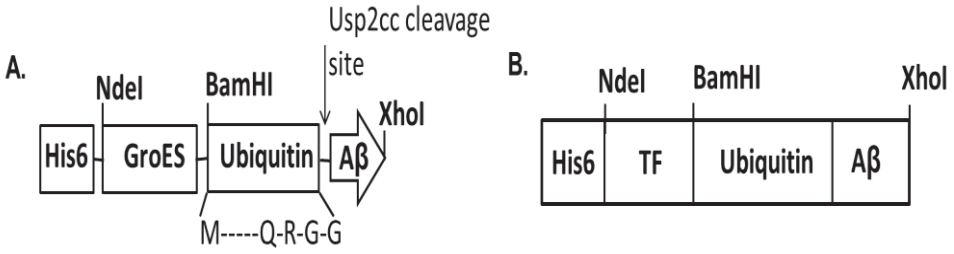

Fig. 1. Schematic representation of the Aβ fusion proteins; (A) GroES-Ub-Aβ42, (B) Trigger factor-Ub-Aβ42.

II-3. Experimental design

The general procedures for the purification of Aβ peptide based on the GroES system are shown in the figure 2A. One key aspect of the protocol is maintenance of the fusion and target protein in a soluble state. Once the inclusion bodies were solubilized by 6 M urea, the proteins stay in solution with the aid of urea during the removal step of the fusion partner protein (His_6-GroES-ubiquitin) and purification steps of the target peptide until it is finally purified, enabling to maintain the concentration of protein high enough, which is advantageous for higher yield of protein.

In the initial protocol, the cleavage reaction mixture of the fusion protein was directly applied to the reverse-phase column. One drawback to the method was the limited amount of the protein applicable to the reverse-phase column, because of the fusion partner protein which comprises a major part of the cleavage reaction mixture and reduces the capacity of the column. More serious problem was that the column performance was deteriorated so rapidly that the column recovery process was frequently necessary. We speculated that the deteriorated performance was due to aggregation of fusion partner protein (His_6-

GroES-ubiquitin) in the column by organic solvent used during the chromatography. Thus, the cleaved fusion partner was removed using His_6 tag at the front of the GroES and conventional Ni-NTA column chromatography before the application to the reverse-phase column. It is critical to increase urea concentration in the chromatography to selectively elute Aβ peptide in the flow through fraction, because the peptide was found to bind the resin of the column in the presence of urea at concentrations lower than 6 M. The procedures for the purification of Aβ peptide based on the TF-ubiquitin system are shown in the figure 2B. The purification method is similarly performed as found in those of the conventional methods.

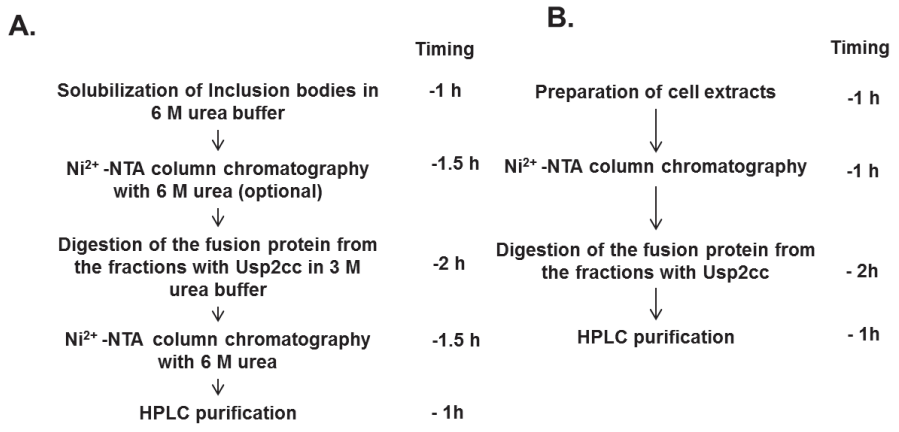

Fig. 2. Schematic step wise representation of the purification system: (A) for inclusion body forming fusion partner (GroES-Ub-Aβ42). (B) for solubilization facilitating fusion partner (TF-Ub-Aβ42).

II-4. MATERIALS AND METHODS

II-4. 1. Reagents

Tris (hydroxymethyl)-amino methane (USB products), Hydrochloric acid (32% W/V), Sodium chloride, Thioflavin-T(Sigma), Glycine, EDTA, Kanamycin (Amresco), Bacto-peptone, Bacto-Yeast extract (Bector, Dickinson and Company), Triton X-100, DTT, β-mercaptoethanol, PMSF, Acetonitrile, Urea, Ammonium acetate, Bradford reagent (Bio-Rad), Acetonitrile (Merck), Ammonium hydroxide, PBS (phosphate buffered saline), Imidazole, HFIP.

II-4. 2. Equipments

- 2 L culture flasks, 250 ml culture flasks,
- 500 ml polyethylene centrifuge tubes,
- Shaking incubator (Jeiotech-SI900R),
- High-speed refrigerated centrifuge (Hanil-Supra 22k),
- Multi-purpose refrigerated centrifuge (Hanil-Union 55R),
- Autoclave,
- iLshin freeze dryer,
- Centrifugal vacuum concentrator (Biotron),
- Ultrasonic cell disruptor (Microson – XL2000),

- AKTA explorer Fast Protein Liquid Chromatography system (Amersham Pharmacia Biotech),
- Hamilton PRP-3 reverse HPLC columns (79147) – (10 μm, 300 Å, 21.2 x 250 mm)
- Preparative Liquid chromatography system (Shimadzu – LC 8A),
- Water bath Sonicator (Branson 8210),
- Ni^{2+}-NTA columns (XK-26 Amersham Pharmacia biotech)
- UV visible spectrophotometer
- Syringe filters (0.22 μM)

II-4. 3. Equipment setup

Equilibration of Ni-NTA columns – XK 26 Ni-NTA columns were connected to an AKTA explorer FPLC chromatography system, equipped with a UV detector and fraction collector and equilibrated with 3 column volumes of (20mM Tris-HCl (pH 8.0), 300mM NaCl, 1mM β-mercaptoethanol and 6M urea) for inclusion body purification step. The upper operational pressure limit was set to 1.8 MPa with the flow rate of 10ml / min.

Equilibration of Hamilton PRP-3 columns for HPLC – Columns were connected to Shimadzu preparative liquid chromatography unit, equilibrated with 3 column volumes of 30 mM Ammonium acetate with 2%

acetonitrile in water for amyloid beta purification. The upper operational limit was set to 22 MPa with the flow rate of 10 ml/min.

II-5. Procedure

II-5. 1. Preparation of large scale culture

1) *Seed culture*

a. BL21 pLysS transformed with pET28-GroES-Ub-Aβ (1-42) or pET28-TF-Ub-Aβ (1-42) was inoculated in each flask containing 50 ml LB media supplemented with kanamycin to a final concentration of 30 μg/ml (in 250 ml flask) x 6 (for 6 L culture).

b. Incubated at 37℃ overnight with shaking at 220rpm.

2) *Large culture*; Volume : 6L(2.4 L flask x 6)

a. seed culture was Spin down at 4000rpm for 10min at 4°C and the supernatant was discarded.

b. cell pellet was added into 1L pre-warmed LB media supplemented with kanamycin to a final concentration of 30ug/ml.

c. Incubated at 37℃ with shaking at a speed of 220 rpm until OD_{600} reaches 0.6-0.8

d. Plasmid expression was induced with 400 μM / L concentration

of IPTG and the culture was further incubated for 4h

3) Harvesting the cells

a. cells were harvested by centrifuging at 4000 rpm for 10 min at 4° C and washed with 50mM Tris-HCl + 150mM NaCl + 5 mM EDTA (20mL/1 L culture)

b. cells were collected in 50ml conical tube by centrifuging at 4000rpm for10min at 4°C

c. cell pellets were stored at -20°C until lysis.

II-5. 2. Preparation of Inclusion bodies, solubilization and Ultra-filtration of soluble protein

1. 20ml of Lysis buffer was added to the cell pellet and resuspended

Lysis buffer: (50mM Tris-HCl (pH 8.0)+150 mM NaCl+5 mM EDTA+0.5% triton X-100+1mM DTT+0.1mM PMSF).

2. Kept in ice for 30min.

3. Cell extract was prepared by using ultra sonic cell disruptor

4. Lysate centrifuged at 10,000rpm for 30minutes

5. Supernatant was discarded and the pellet was saved

6. Then the pellet was washed with *Washing buffer I* for 3 times (50mM Tris-HCl (pH 8.0) + 150mM NaCl + 5 mM EDTA + 0.5%

triton X-100 and 1mM DTT).

7. Wash the pellet with *Washing buffer II* (50mM Tris-HCl (pH 8.0) + 150mM NaCl + 5 mM EDTA + 1 mM DTT) twice. Inclusion bodies were collected by centrifugation at 10,000rpm for 30minutes.
8. The pellet was stored in -20~-70 for the later use.

II-5. 3. Solubilization

1. 20ml/L of solubilization buffer was added and incubated for 30minutes at room temperature.

   Solubilization Buffer: 50mM Tris-HCl, 150mM NaCl, 2mM β-mercaptoethanol, 6M Urea
2. Soluble proteins were collected by centrifugation at 18000 rpm for 30minutes.

II-5. 4. Purification of Inclusion body using Ni2+-NTA column chromatography

1. Before injecting the soluble proteins into the column, the column was equilibrated with 3 column volumes of Buffer A - (20mM Tris-HCl (pH 8.0), 300mM NaCl, 1mM β-mercaptoethanol and

6M urea).

2. Then the soluble proteins were injected in to the column at the flow rate of 10ml / min, Flow through was collected for further analysis.
3. After the soluble protein injection, the column was washed with 3 column volumes of Buffer A at the flow rate of 10ml / min.
4. For elution, 6 column volumes of Buffer B - (200mM NaH_2PO_4 (pH 4.0), 10mM Tris-HCl, 1mM β-mercaptoethanol, 6M urea) was used and fusion proteins have been collected.

II-5. 5. Digestion of GroES-Ubiquitin-Aβ (1-42) fusion protein with Usp2cc enzyme

1. The protein samples were diluted 3-times in Buffer A and urea added accordingly to maintain the final concentration of 3M to avoid precipitation of fusion protein (keep protein concentration up to 4-5mg/ml) immediately before digestion.
2. For digestion, a final concentration of 2mM β-mercaptoethanol and Usp2cc enzymes at 1:50 weight ratio (enzyme : substrate) or a 1:100 molar ratio was added and incubated at 37°C for 2hrs.
3. After incubation, the digested protein sample was sonicated on

water bath for 10min followed by centrifugation at 18,000rpm for 30 minutes

4. Save supernatant for the next step purification

II-5. 6. Purification of Aβ (1-42) using Ni^{2+}-NTA column chromatography

1. Urea concentration of the protein sample was increased to 6M prior to Ni^{2+} column injection.
2. The column was equilibrated with 3 column volumes of Buffer A (20mM Tris-HCl (pH 8.0), 300mM NaCl, 1mM β-mercaptoethanol and 6M urea.
3. Digested fusion proteins were injected in to the column at the flow rate of 10ml / min, Flow through was collected and kept on ice.
4. After the sample injection, the column was washed with 3 column volumes of Buffer A at the flow rate of 10ml / min.
5. For elution, 4 column volumes of Buffer B (20mM Tris-HCl (pH 8.0), 300mM NaCl, 1mM β-mercaptoethanol, 6M urea and 250 mM Imidazole) was used and the fractions were collected for

further analysis.

II-5. 7. HPLC: Separation of amyloid beta peptide on polymer based column

1. Reverse phase chromatography column was equilibrated with 3 column volume of Buffer A and Aβ containing Ni^{2+} column fractions were injected on to the column. (loaded 100mg total protein per injection)
2. The column bound Aβ peptide was eluted with a gradient of HPLC B buffer over 60 minutes.

   Column: Hamilton PRP3 (79147) – (10 μm, 300 Å, 21.2 x 250 mm)

   Flow rate: 10ml/min

   HPLC buffer A: 10mM Ammonium acetate, pH 10 in 2% acetonitrile

   HPLC buffer B: 70% acetonitrile

   Gradient: Linear 0-20% buffer B over 5 minutes. Then 20% - 40% B in 30minutes and 40% - 100% B for next 30 minutes.
3. Peptide fractions were collected in 50ml conical tube and

lyophilized.

II-5. 8. Purification of Aβ (1-42) fused with Trigger factor-Ubiquitin

1. E.Coli cells transformed with pET28-TF-Ub-Aβ (1-42) vector were overexpressed and harvested by centrifugation at 4000 rpm for 10 min at 4°C.
2. Cell pellets were lysed with 20mM Tris-HCl (pH 8.0), 10mM NaCl, 0.1 mM EDTA, 1mM β-mercaptoethanol) and centrifuged at 20,000 rpm for 1h.
3. The soluble fraction was applied to a Ni-NTA column equilibrated with 3 column volumes of Buffer A (50mM Tris-HCl, pH(8.0), 150mM NaCl, and 1mM β-mercaptoethanol).
4. Then the column was washed with 5 column volumes of Buffer A and the protein was eluted with Buffer B (Buffer A+250 mM imidazole).
5. Fractions containing fusion proteins were quantified, diluted 2-fold and incubated with Usp2cc enzyme in 1:100 enzyme-protein molar ratio at 37°C for 2h.
6. The samples were then centrifuged and subjected to preparative

reversed-phase HPLC with a solvent system buffer A (30mM ammonium acetate, pH 10.0, and 2% acetonitrile) and buffer B (70% acetonitrile in water) at a flow rate 10ml/min using a 20% - 40% linear gradient over 35 mins

7. Peptide fractions were collected in 50ml conical tube and lyophilized.

II-5. 9. Aliquoting and Storage

1. The purified peptides were weighed and dissolved in 100% 1,1,1,3,3,3-hexafluoro-2-propanol (HFIP) at a concentration of 0.5 to 1 mM and sonicated in water bath until the peptide solution becomes clear.
2. A small quantity of clear peptide solution was dried under vacuum and suspended in 0.1% NH4OH and the concentration of peptide measured by BCA method.
3. 0.5 mg aliquots were made in an sterile tube, vaccum dried to evaporate HFIP and stored at -20°C.

II-5. 10. Aggregation kinetics using thioflavin (ThT) binding assay

1. Each Aβ was dissolved in PBS (300 μl) and allowed to aggregate at 37 °C for the indicated time without shaking.

2. At the end of the reaction, 20 μl of the reaction mixture was mixed with 80 μl of 5 μM ThT in PBS solution

3. fluorescence was measured immediately at an excitation of 445 nm and emission of 490 nm using the Microplate Spectrofluorometer Gemini-XS (Molecular Devices, Sunnywale, CA) [69].

4. The plot of Aβ ThT fluorescence vs. time followed a characteristic sigmoidal shape, as described previously [69].

To estimate $t_{½}$ (time to reach half maximal ThT fluorescence calculated using the following equation), straight lines resulting from a plot of Log$\{F(t)/[F(\infty)-F(t)]\}$ vs. time were fitted by $at+b$, where t is reaction time, $F(t)$ is the fluorescence as a function of time, and a and b are the slopes and y-intercepts of the lines, respectively [69] . Because $F(t_{½})$ is $F(\infty)/2$ or Log$\{F(t_{½})/[F(\infty)-F(t_{½})]\}$ is 0, as defined, $t_{½}$ is $-b/a$, where a and b can be obtained from

the plot. The rate of fluorescence increase (or rate of polymerization of ThT-binding aggregates) is highest at time $t_{½}$ [69]. On the other hand, T_{50} is time to reach half maximal ThT fluorescence estimated from the plot without using an equation.

II-6. RESULTS AND DISCUSSION

The summary for the purification result are shown in figure 3. We initially purify wild-type Aβ42 (Aβ42wt), but this method was applicable to purify other Aβ variants such as Dutch Aβ42 (Aβ42Du), Flemish Aβ42 (Aβ42Fl), wild-type Aβ40 (Aβ42wt), Dutch Aβ40 (Aβ40Du) and Flemish Aβ40 (Aβ40Fl). The yields were varied from ~2 mg/l of culture (Aβ42Du) to ~15 mg/l of culture (Aβ42wt).

Inclusion of optional step of Ni-NTA chromatography in the GroES system produced more pure the fusion protein which may facilitate the cleavage, but took more step and time and reduced the yield almost by half (figure 3A vs. 3B). Thus, omission of the step is beneficial if the cleavage step can be carried out efficiently enough. Purification of Aβ42 using the TF system was easier to be performed, because the solubilization step was not necessary. The purified Aβ42 showed no detectable difference from the peptide of the GroES system, but the yield was a little low (~8 mg/l of culture).

The GroES system was advantageous over the above TF system in several aspects for purification of Aβ peptide, because if the target was insoluble after the cleavage as observed in Aβ peptide preparation, purification of the targets after cleavage of the fusion partner protein would be difficult in the TF system, because the heterogeneous species generated during the aggregation process made it difficult to purify the pure target, resulting in lower yields (data not shown). Further advantages of the GroES system were that (i) preparation and storage of inclusion bodies were easier than preparation of cell extract; (ii) the target protein contents were higher in inclusion bodies which facilitate the next purification; (iii) yield was higher. For these reasons, we prefer the GroES system to the TF soluble system for purification of Aβ. However, the TF-ubiquitin system was useful in purification of other inclusion body-forming proteins which are prone to lose their activity when they form the inclusion bodies and are needed to maintain folded state after the cleavage. Thus, the present protocols for both systems, enabling researchers to select a method suitable for their target proteins, although only Aβ purification procedures are provided here.

Aggregation kinetics data of the newly prepared Aβ were compared

with those of other preparations reported previously. $t_{½}$'s for Aβ42wt, Aβ42Du and Aβ42Fl were ~1.4, ~2.1 and ~0.8 h, respectively, while $t_{½}$'s for Aβ40wt, Aβ40Du and Aβ40Fl were ~21, ~45 and ~7.7, respectively. It is difficult to compare the fibrillogenic results obtained in the current study to those from other groups, because of the huge differences depending on the reports. For example, $t_{½}$ or T_{50} of Aβ40wt varied from 107 min [68] to ~24 h [41] and that of Aβ42wt from 18.7 min [69] to ~24 h [70]. T_{50} of Aβ40Du also varied from 59 min[68] to ~6 h [71], while it was ~3 h for Aβ42Du[72]. More confusing estimations were reported for the Flemish variants. T_{50} of Aβ40Fl was ~2-50 h[68], while Aβ42Fl poorly formed ThT-binding aggregates in another report [72] . Because of the variable values of T_{50} or $t_{½}$ in previous reports, it is difficult to evaluate the peptides prepared in the current study by simple comparison of the fibrillogenic parameters.

Meanwhile, Aβ preparations showed the general characteristics of wild-type and variant Aβ peptides: higher amyloidogenic property of Aβ42 than Aβ40, faster aggregation rate for the Dutch variants, and slower rate for the Flemish variants compared to the wild-type. In addition, biophysical properties such as mass, elution profile in high

performance liquid chromatography and formation of β-sheet assayed by circular dichroism spectroscopy in the previous [73] and current (data not shown) studies all validate our preparations as a reliable resource for these investigations

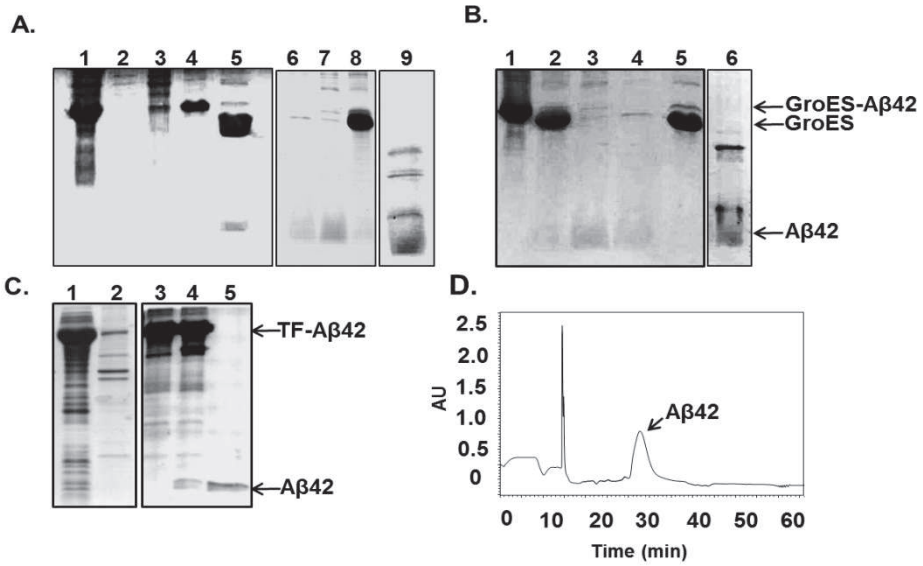

Fig. 3. Purification of Aβ42 from different fusion partners (A) SDS-PAGE (15%) analysis of Aβ42 and its fusion proteins from two step Ni column purification. Lanes: 1, Inclusion body contains GroES-Ub-Ab42 fusion protein; 2 and 3, Flow through and Buffer A wash fractions of Ni-NTA column; 4, Ni column fraction contains fusion protein; 5, the fusion protein digested by Usp2cc; 6 and 7, Flow through and Buffer A wash fractions of Ni column containing cleaved Aβ42 peptide; 8, Ni column fraction containing GroES; 9, HPLC pure Aβ42. (B) SDS-PAGE analysis of one step Ni column purification. Lanes: 1, Inclusion body contains GroES-Ub-Ab42 fusion protein; 2, Usp2cc digested fusion protein; 3 and 4, Flow through and Buffer A wash fractions of Ni column containing Aβ42; 5, Ni column fraction containing GroES; 6, HPLC pure Aβ42. (C) SDS-PAGE analysis of Trigger factor-Ubiquitin- Aβ42 fusion protein. Lanes: 1, Soluble fraction of fusion protein expressed cell lysate; 2, insoluble fraction of cell lysate; 3, TF-Ubiquitin-Aβ42 fusion protein purified from Ni-NTA column; 4, the fusion protein digested by Usp2cc; 5, HPLC purified Aβ42 peptide. (D) Chromatogram shows elution profile of reverse-phase HPLC.

III. Construction and purification of FLAG-Aβ42

III-1. INTRODUCTION

To identify the amyloid beta interacting cellular proteins, it is necessary to use a good protein complex isolation system. Especially when we use antibody based pull down assay the specificity of the antibody to its target is very important. We utilized immunoprecipitation method during this study; we found some difficulties with amyloid beta antibodies specificity. To overcome this problem and to improvise the amyloid beta antibody binding efficiency, we designed FLAG tagged Aβ42 system. The FLAG system utilizes a short, hydrophilic 8 amino acid peptide (Asp-Tyr-Lys-Asp-Asp-Asp-Asp-Lys) which can be fused to the recombinant protein of interest. The FLAG peptide includes the binding site for several highly specific Anti-FLAG monoclonal antibodies (M1, M2, M5). The FLAG peptide is likely to be located on the surface of a fusion protein because of its hydrophilic nature, as a result it is more likely to be accessible to antibodies. In addition, because of the small size, the peptide is not likely to obscure other epitopes, domains or transport of the fusion protein [74]. It can be used in affinity chromatography to separate overexpressed recombinant protein, It can

also be used in the isolation of protein complexes with multiple subunits.[74, 75, 76]

III-2. MATERIALS AND METHODS

III-2. 1. Construction and purification of FLAG tagged amyloid beta peptides

Genes encoding GroES, Ubiquitin and Aβ42 were PCR amplified, cloned between NdeI and BamHI sites of pET28b expression system, whereas FLAG tagged Ab42 was synthesized by inserting FLAG sequence between ubiquitin and Ab42 sequence using antisense primer 5'-GTGTTGCGCCTCCGCGGTGGAGATTACAAGGATGACGATGACAAG GATGCAGAATTCCGACATGAC -3' and sense primer 5'-GTCATGTCGGAATTCTGCATCCTTGTCATCGTCATCCTTGTAATCTC CGCGGAGGCGCAACAC -3'. The fusion protein was overexpressed as inclusion bodies in *E.coli* BL21 (DE3) pLysS cells and isolated. Inclusion bodies were solubilized in a buffer containing 6M urea and digested with Usp2cc. Digested FLAG-Aβ42 samples were injected in the Ni-NTA column for first step purification to remove the co-expressed fusion protein. Then FLAG-Aβ42 containing flow through and Buffer A wash

fractions were pooled and subjected to reverse phase HPLC. HPLC pure FLAG-Aβ42 were lyophilized and stored at -20°C until use.

III-2. 2. Immunoprecipitation

250μg of HeLa cell extracts were incubated with 0 and 20uM concentrations of FLAG-Aβ42 for 6h at 37 ^{o}C. Following incubation mouse monoclonal antibodies for FLAG peptide were added to the reaction mixture and kept at 4°C for overnight. Next 20-40 μl of Protein A Sepharose (Amersham Biosciences, Uppsala, Sweden) beads were added to each sample and incubated at 4°C for 2h. Beads were precipitated by centrifuging at 13000 rpm at 4°C for 5 min and washed 3 times with PBS. 15 μl 2X SDS loading buffer was added to the beads, boiled for 5 min and centrifuged at 13000rpm for 10 min. The obtained supernatants were then analyzed by SDS-PAGE and immunoblotting.

To analyze random and non-specific interaction of FLAG- Aβ42 with Protein A Sepharose beads, 100ug aliquots of FLAG- Aβ42 were incubated with or without beads and anti-FLAG antibodies at 4°C for overnight. After incubation, the beads were precipitated at 13000 rpm for 10 min at 4°C. Then the supernatant and bead precipitates were boiled and resolved through SDS-PAGE and immunoblotted for FLAG peptide.

III-2. 3. Immunocytochemistry

HeLa cells were seeded in 12 well plates at 70% confluency, cultured for 24h and further incubated for 12h in serum free media and then treated without or with 20 or 40 μM FLAG-Aβ42. Harvested cells were fixed in methanol at -20 ^{o}C and permeabilized by 0.3% Triton X-100. After blocking with 0.1% BSA overnight, mouse anti FLAG (M2) and rabbit anti caspase-9 antibodies were added and incubated overnight at 4°C. After washing with PBS Alexa-Flour-488 conjugated chicken anti-mouse IgG and Alexa Fluor-543 conjugated chicken anti-rabbit IgG antibodies were treated for 2h at room temperature followed by PBS washing. Nuclei were stained with Hoechst and confocal images were obtained with a Carl Zeiss LSM510 microscope using the vendor provided software (LSM510).

III-2. 4. RESULTS AND DISCUSSION

The fusion protein module that contains GroES, Ubiquitin, FLAG, and Aβ42 were overexpressed as inclusion bodies in E.Coli based expression system. The molecular mass of the peptide were confirmed by Mass spectrometry which shows the expected 5507.5 Da. Next, we determined to test whether the FLAG- Aβ42 binds or interacts non-

specifically (in the absence of antibody) to the beads which may leads to false positive results. To analyze this, FLAG- Aβ42 were incubated with or without the beads and FLAG antibody at 4°C for overnight. The beads and the supernatant were obtained by centrifugation, resolved through SDS-PAGE and immunoblotted for FLAG peptide. The results shown FLAG- Aβ42 did not precipitate with the beads in the absence of FLAG peptide antibodies.

We further tested whether the FLAG tagged Aβ42 still binds its intracellular targets like procaspase-9 by incubating 20uM FLAG-Aβ42 with 250 µg of HeLa cell extract at 37 ^{o}C for 6 h and immunoprecipitated with monoclonal antibody (M2) for FLAG peptide, then immunoblotted for Caspase-9 with rabbit polyclonal anti caspase-9. The results shown, Caspase-9 co-immunoprecipitated with FLAG- Aβ42 which suggests that the binding property of Aβ42 remains intact. Confocal images of Wild type Aβ42 treated HeLa cells shown the interaction between caspase 9 and Aβ42.(Fig. 6C).

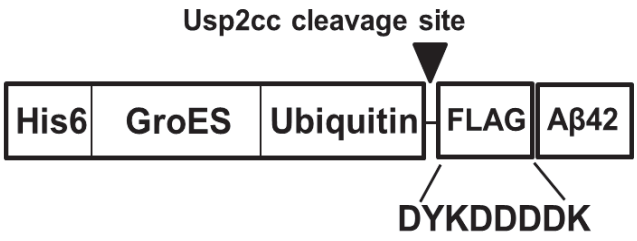

Fig.4. Schematic representation of the FLAG-Aβ42 construct

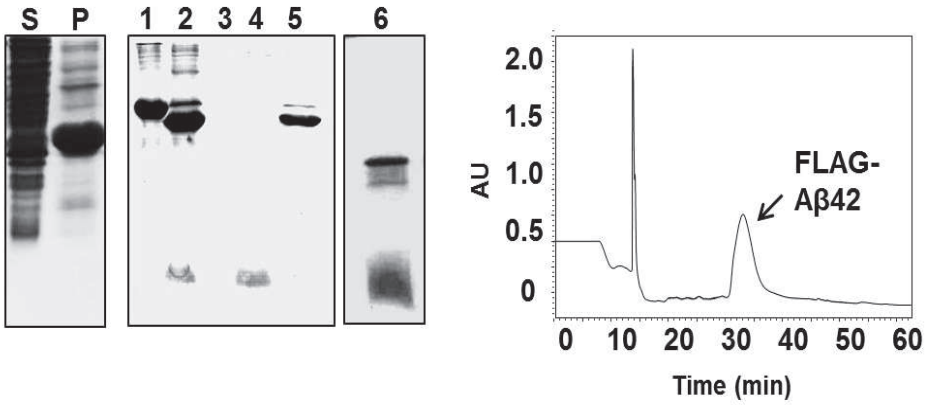

Fig. 5. Expression and purification FLAG-Aβ42 (A) SDS-PAGE analysis of overexpressed GroES-Ub- FLAG-Aβ42 fusion protein. Lanes: (S) soluble fraction and (P) insoluble fractions of bacterial cell lysate. 1, Inclusion body of GroES-Ub- FLAG-Aβ42 fusion protein; 2, Fusion protein digested by Usp2cc; 3 and 4, Ni-NTA column fractions containing FLAG-Aβ42; 5, Ni column fraction containing part of the GroES fusion protein; 6, HPLC pure FLAG-Aβ42. (B) HPLC chromatogram shows elution profile of FLAG-Aβ42.

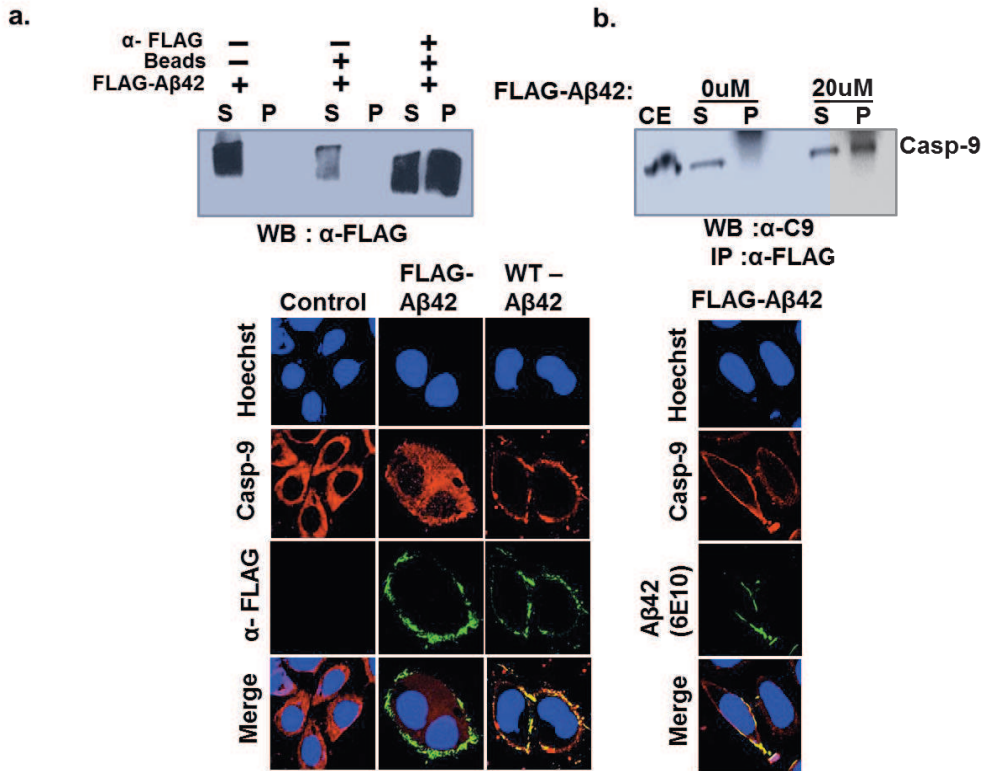

Fig. 6. Immunoprecipitation and confocal analysis of FLAG- Aβ42 (A) Western blot analysis of FLAG- Aβ42 incubated with or without Protein A Sepharose beads and anti-FLAG antibodies. (B) HeLa cell extracts were incubated with 0 and 20 μM concentrations of FLAG-Aβ42 for 6h, immunoprecipitated with anti-FLAG and immunoblotted for Caspase-9.(C) HeLa cells treated with 20 μM FLAG- Aβ42 and wild type Aβ42. Primary mouse anti-FLAG or mouse anti- Aβ (6E10) and rabbit anti-caspase-9 antibodies in addition to secondary anti-mouse IgG-FITC and anti-rabbit IgG Rhodamine antibodies were used to detect intracellular Aβ (green) and Caspase (9) respectively. Nuclei were seen Hoechst nuclear stain. Images visualized using Carl-Zeiss confocal microscope (LSM510).

IV. Identification of nuclear scaffold protease modulating β-amyloid-induced cell death by screening protease inhibitors

IV-1. INTRODUCTION

Cell death process involves diverse signal pathway and many factors [78]. Among those death factors, proteases play pivotal roles in several types of cell death process. We have a hypothesis that different types of proteases are activated according to the type of cell death or cell death-inducing agent.

Caspase is one of well-known proteases related to cell death [44]. The apoptotic enzyme is synthesized as a zymogen form which is activated by apoptotic signal. Among the two well-defined apoptotic pathways, receptor-mediated apoptosis, or extrinsic apoptosis is characterized by the formation of the death-inducing signaling complex (DISC). On the other hand, chemical-induced apoptosis or caspase-dependent intrinsic apoptosis leads to mitochondrial damage, resulting

in the release of cytochrome c which associates with caspase-9, dATP and an adaptor protein Apaf-1 to form a multiprotein complex called apoptosome. The DISC and apoptosome complex activate procaspase-8 and procaspase-9, respectively. Once activated, caspase-8 and -9 then process effector caspases, including caspase-3, -6 and -7 which are responsible for most of the cleavage events observed during apoptosis. Beside the two apoptotic pathways, endoplasmic reticulum stress involved in neurodegenerative disease including Alzheimer's disease induces caspase-4 activation by the unfolded protein response signaling pathway [45].

Other proteases than caspases have been identified to participate in the death process. For example, a mitochondrial serine protease Omi/HtrA2 is released in the cytosol, where it contributes to apoptosis through both caspase-dependent and -independent pathways [46]. It proteolytically removes not only natural inhibitors of caspase such as XIAP and cIAP1 to assist caspase activation, but also many other target proteins which might mediate caspase-independent apoptosis. Lysosomal cathepsin proteases are other example for death-inducing protease. They are released to cytosol by a process known as lysosomal membrane permeabilization [48]. The proteases in cytosol

can induce both caspase-dependent and –independent cell death. The calcium-dependent proteases, calpains, have been also implicated in cellular apoptotic processes [49]. The proteases process several members of the Bcl-2 family of cell death regulators and caspases [50]. The ubiquitin-proteasome system also contributes to cell death [50]. Besides those exemplified proteases, other proteases such as matrix metalloprotease, aminopeptidase and have been suggested to play a critical role in apoptosis or other cell types of cell death [51].

In the current study, we made an attempt to correlate specific protease(s) to selected cell death-inducing agent. Particularly, non-caspase proteases functioning in the cell death were interested, because roles of the enzymes in the death process are relatively less understood. β-amyloid (Aβ), a hallmark peptide of Alzheimer's disease (AD), was chosen as a death inducer, because it is important in pathogenesis of the disease, and its cell death inducing mechanism_is not well understood: caspase-independent process as well as caspase-mediated apoptotic process seems to be involved in the cell death. Aβ is 36-43 amino acid-long peptides generated by proteolytic cleavage of the amyloid precursor protein by α-, β- and γ- secretases [1-3]. The

conformation of Aβ peptides spontaneously alters to β-sheet-rich unstable intermediate structures which interact with each other to form aggregates such as oligomers, profibrils and fibrils [12-13]. The aggregated Aβ progressively deposits in brain parenchyma and cerebral blood vessels [79]. Recent evidences suggest that soluble Aβ oligomers and protofibrils more toxic than the fibrils would be the main factor for AD are accumulating [17-20].

Although it is not yet clearly understood which plays a major role in the cell death process induced by Aβ, involvement of apoptosis in the process has been proposed, because caspases are activated upon administration of the peptide to cells. A number of reports indicate that both caspase-8 (extrinsic pathway) and caspase-9 (caspase-dependent intrinsic pathway) are activated in Aβ-treated cells. The differential activation of each pathway might depend on the conformational states of Aβ (oligomer vs. fibril) [79]. It is also possible that binding of Aβ to p75 neurotrophin receptor can trigger the extrinsic pathway, while the mitochondrial dysfunction caused by the peptide can trigger the intrinsic pathway. Beside the two apoptotic pathways, caspase-4-mediated apoptosis is also induced by the unfolded protein response signaling pathway when endoplasmic reticulum stress is prolonged. Aβ seems to

induce caspase-independent cell death pathway, too. One report supporting for existence of the pathway indicates that pharmacological inhibition of caspase activity could not prevent Aβ-induced cell death, although it could block caspase activation [80].

In the present study, to identify protease(s) playing a role in Aβ-induced cell death commercially available protease inhibitors were screened for inhibition of the cell death. For comparison, the protease inhibitor screening (PIS) method was also applied in the similar way for cell death induced by staurosporine (STS) which causes the well-defined caspase-dependent intrinsic apoptosis. We could successfully identify a protease inhibitor which suppresses Aβ-induced cell death but not STS-induced cell death. It is an NS protease inhibitor which was further explored to define the role of the protease in Aβ-induced cell death.

IV-2. MATERIALS AND METHODS

IV-2. 1. Materials

Fetal Bovine serum (FBS) was purchased from Life Technology Inc. (Grand Island, USA). Dulbecco's modified Eagles medium, Ham's F

12(1:1) (DMEM/F-12) and high glucose (DMEM/HG) were obtained from Welgene (Daegu, Korea). Caspase-9, Caspase-8, Caspase-6 and Caspase-3 substrates, N-acetyl Leu-Glu-His-Asp-amino methyl coumarin (Ac-LEHD-AMC), Ac-IETD-AMC, Ac-VEID-AMC and Ac-DEVD-AMC, respectively, were from A.G. Scientific Inc. (San Diego, USA), Caspase inhibitor Z-VAD-FMK from Alexis (Lausen, Switzerland). Ni-NTA column were purchased from Amersham Biosciences (Piscataway, USA). Western blotting detection kit (WEST-ZOL PLUS) from iNtron Biotechnology (Gyeonggi-do, Korea). Phosphate buffer saline (PBS) purchased from Amresco (solon, USA). Monoclonal anti-Aβ antibody 6E10 was acquired from Signet Laboratories (Dedham, USA), anti-caspase-9, anti-caspase-3, anti-lamin-A/C, anti-lamin b and anti-β-actin from Santa Cruz Biotechnology (California, USA), anti-caspase-8 from Cell Signaling Technology (Massachusetts, USA), anti-DFF45 from BD Transduction Laboratory (San Diego, USA) and anti-Bid developed in laboratory. Polyclonal antibody anti-caspase-9(p10) obtained from SantaCruz Biotechnology, Urea was from USB chemicals, Acetonitrile from Merck (Darmstadt, Germany). All other chemicals obtained from Sigma (St. Louis, USA), unless otherwise stated.

IV-2. 2. Preparation of Aβ42

The purified peptide was solubilized in 100% 1,1,1,3,3,3,-hexafluoro-2-propanol, and dried under nitrogen flow and subsequently, under vacuum for 30 min. The peptide aliquots were stored at –20 °C until use. Immediately before use, the peptide was dissolved in 0.1% NH_4OH at a concentration of 2 mg/ml followed by bath sonication for 10 min. The solution was diluted at the desired concentration with PBS. Aβ42 oligomers were prepared as described earlier [108] with little modification. Briefly, peptides were diluted in cell culture media at 100 μM concentration, vortexed for 30 seconds and incubated at 4°C for 12 h. The peptide solution then diluted to the desired concentrations. To make fibrils, Aβ42 (100 μM) was incubated in presence of 0.02% sodium azide in PBS at 37 ^{o}C for 4 days. The samples were centrifuged at 16000 x g for 30 mins. Pellet fraction (fibrils) was washed three times with PBS. Fibrils were sonicated for 10 min, quantified by Branford method and used immediately or stored at -80 ^{o} C.

IV-2. 3. Cell Culture and Cytotoxicity Assay

Human epithelial HeLa cells were cultured in DMEM (High glucose) medium supplemented with 10% (v/v) FBS and 1% antibiotics at 37 °C

under 5% CO_2.

For MTT cytotoxicity assay, cells were plated at a density of 15,000 cells/well in 96-well plates (Nunc, Denmark) and cultured for 24 h followed by serum deprivation for another 12 h. Cells were exposed to the Aβ preparation for 12 - 24 h and the viability was assessed by 3-(4,5-dimethylthiazol-2-yl)-2,5-di-phenyltetrazolium bromide (MTT) reduction test. Briefly, 20 μl of 5 mg/ml MTT solution in PBS was added to each well and incubated for 2 h. Then 100 μl of solubilization buffer [20% SDS solution in 50% (v/v) DMF (pH 4.7)] was added. After 12-16 h of incubation, absorbance was recorded at 570 nm using a micro plate reader Spectra Max 190 (Molecular Devices, CA, USA).

For Alamar blue assay also same cell culture and treatment method was followed. After treatment 10 μl of alamar blue (Life technologies) was added directly to the cells and incubated for 4-16 h, absorbance was recorded at 570 nm using a micro plate reader Spectra Max 190 (Molecular Devices, CA, USA).

IV-2. 4. Measurement of Caspase activity

Caspase activity was measured as described earlier [109].

Briefly, treated cells were washed twice with ice-cold phosphate-buffer saline (PBS). Then, 40 μl of buffer containing 20 mM HEPES-NaOH, pH 7.0, 1mM EDTA, 1mM EGTA, 20mM NaCl, 0.25% Triton X-100, 1mM dithiothreitol (DTT), 1mM phenylmethanesulphonylchloride (PMSF), 10 μg/ml leupeptin, 5 μg/ml pepstatin A, 2 μg/ml aprotinin, 25 μg/ml ALLN was added into each well and incubated on ice for 20 min. Caspase assay buffer (final 20mM HEPES-NaOH, pH 7.0, 20mM NaCl, 1.5 mM $MgCl_{2,}$ 1mM EDTA, 1mM EGTA and 10mM DTT) was added and the release of AMC was monitored for 2h in 2 minute interval with final with respective caspase substrates at excitation and emission wavelengths of 360 nm and 480 nm respectively, using microplate sepectrofluorometer (Molecular Devices, CA, USA). The results were expressed as a slope of total readings versus time.

IV-2. 5. Protease inhibitor screening (PIS)

MTT assay was used to screen the protease inhibitors that can inhibit the cell death induced by Aβ42 or STS. Cells were plated at a density 15,000 cells/well in 96 well plate and cultured for 24 h followed serum deprivation for another 12 h. cells were exposed to Aβ or STS in the presence or absence of protease inhibitors, z-VAD-FMK (20 μM),

Suc-AAPF-CMK (40 μM), ALLN (Calpain inhibitor, 20 μM), MG132 (Proteasome inhibitor, 5 μM), leupeptin (20 μM), Roscovitine (Cdk5 inhibitor, 5μM) and the viability was assessed by 3-(4,5-dimethylthiazol-2-yl)-2,5-di-phenyltetrazolium bromide (MTT) reduction test as described earlier.

IV-2. 6. Measurement of Nuclear Scaffold protease assay

NS protease activity was measured as described earlier . Briefly, treated cells were washed twice with ice-cold phosphate-buffered saline (PBS). Then, 40 μl of buffer containing 50 mM Tris-HCl (pH 7.5), 25 mM KCl, 5 mM $MgCl_{2,l}$ 0.5% Triton X-100, 0.5% Nonidet p40 (NP40), 1 mM DTT, 10 μM EDTA, 10 μM E64 was added into each well and incubated on ice for 10-20 mins. NS assay buffer (final 50 mM Tris-HCl, pH 7.5, 100 mM KCl, 5 mM $MgCl_2$ 10 μM $CaCl_2$ 1 mM DTT, 10 μM E64 was added and the release of AMC was monitored for 2h in 2 minute interval with final concentration of 250 μM Suc-AAPF-AMC substrate at excitation and emission wavelength of 360 nm and 480 nm respectively, using Microplate Spectrofluorometer (Molecular Devices, CA, USA). The results were expressed as a slope of total readings versus time.

IV-2. 7. Western blot analysis

Cells were harvested, washed with ice-cold PBS and resuspended in lysis buffer (50 mM Tris-HCL, pH 8.0, 150 mM NaCl, 1% Triton X-100, 5mM EDTA, 5mM EGTA, 1mM PMSF, 10 μg/ml leupeptin, 2 μg/ml pepstatin A and 2 μg/m aprotinin) for 20 min on ice. The extract was obtained by centrifugation at 14,000 rpm at 4°C for 15 min. The amount of protein was measured through Bradford assay. Equal amounts of proteins were separated on 12–15 % SDS-PAGE and transferred on to a PVDF membrane. The membrane was immunoprobed with primary antibodies and horseradish peroxidase-conjugated secondary antibodies. The blots were visualized using West-Zol plus reagent (iNtron Biotechnology Inc,, Seoul, Korea).

IV-2. 8. Immunocytochemistry

HeLa cells were seeded in 12 well plate at 70% confluency, cultured for 24h and further incubated for 12h in serum free media and then treated without or with 40 μM Aβ42 in the presence or absence of Caspase (z-VAD-FMK), NS protease (Suc-AAPF-CMK), Cyclin dependent kinase (Roscovitine) inhibitors for 4+6h. Treated cells were fixed in methanol at -20 ^{o}C and permeabilized by 0.3% Triton X-100.

After blocking with 0.1% BSA overnight, goat anti lamin A/C and lamin B polyclonal antibodies were added to each samples and incubated overnight at 4°C. After washing with PBS, Alexa-Fluor-543 conjugated rabbit anti-goat IgG antibodies and Alexa-Flour-488 conjugated rabbit anti-goat IgG antibodies (dilution, 1:200) were treated for 2h at room temperature followed by PBS washing. Nuclei were stained with Hoechst and confocal images were obtained with Carl Zeiss LSM510 microscope (Jena, Germany) using vendor provided software (LSM 510).

RESULTS and DISCUSSION

IV-3. Searching for condition in which cell death occurs without caspase activation in Aβ42-treated cells

One prime purpose of this study was to identify caspase-independent protease which is activated in Aβ42-treated cells. For the purpose, initially cell treatment conditions were sought out in which Aβ42-induced cell death occurs without caspase activation. It was also important to find a condition under which cell survival was minimally affected by the protease inhibitor alone for application of PIS method to the aim (see below). Human epithelial HeLa cells were mainly employed for this study, because it was previously observed that these cells are relatively resistant to toxicity of protease inhibitors shown below (data not shown). Cell lines such as human neuroblastoma SH-SY5Y cells also considered, but death occurred too easily under the most conditions tested and the levels of activated caspase were inconsistent (data not shown). And only oligomeric preparation of Aβ42 was used for the experiment instead of monomeric or fibrillar peptide. Otherwise indicated, Aβ42 indicates oligomeric peptide in the followings.

4 different synthetic substrates (DEVD-AMC, VEID-AMC, IETD-

AMC, and LEHD-AMC for each caspase, respectively) were employed to check the activity of caspase-3, -6, -8 and -9 which plays an essential role in the extrinsic and intrinsic caspase-dependent apoptotic pathways [44]. Aβ has been reported to induce those apoptotic pathways [79]. The substrates, however, are not specific for the corresponding caspase (ref). For example, caspase-3 shows optimal activity with DEVD-AMC, but also has a substantial activity with VEID-AMC (ref). In this study, therefore, the activity with DEVD-AMC is expressed by caspase-3-like activity, if necessary.

Cell death was assessed by the 3-(4,5-dimethylthiazol-2-yl)-2,5-diphenyltetrazolium bromide formazan (MTT) assay. The assay has been questioned as a reporter of Aβ-mediated cell death in a previous report (ref), because soluble Aβ can lead to a decrease in MTT formazan production in the absence of overt cell death when cells are incubated for longer time (ref). However, the cell death estimated using alamarBlue assay (ref) produced comparable results (data are shown only in figure 8). Furthermore, the decrease of MTT formazan was low as shown in the 12-h incubated cells (figure 1E), indicating that the decrease by Aβ was negligible. In the following experiments, treatment for less than 12 h was mainly used. Thus, we conclude that MTT assay

is a valid method for cell death measurement in the current study.

Enzyme activities for the 4 substrates were not perceivable and the cell death was less than 20% in the cells treated for 12 h with Aβ42 at all tested concentrations up to 40 μM (Fig 7A-D and 7E). Thus, the 12-h incubation was not adequate for the following experiments because of the low cell death levels. In cells treated with the same amount of the peptide for 24 h, certain levels of activities, especially with IETD-AMC and LEHD-AMC, were observed, although they were low compared to those activated by other apoptogen such as STS (data not shown) or the double treatment (see below). 24-h incubation was not applicable for the following study either, for a certain level of caspase activity was detected and the levels of cell death was barely prominent (figure 7A-D).

For the study we search for ~30~40% cell death condition, but it was not sufficient in the “single” treatment experiments. Although cells incubated for more than 24 h showed that levels of death (data not shown), the longer incubation often induced robust activation of caspase (data not shown). Thus, to find condition where cell death occurs rather quickly, we next tested “double treatment” method in which Aβ42 peptide was sequentially twice administered to cells, referring to a report

that nucleation-dependent polymerization is an essential for Aβ-mediated cell death [81]. Cells were initially treated for 4 h with the indicated concentration of Aβ42 which then was removed at the end of incubation and subsequently, were further incubated with new preparation of Aβ42 peptide at the same concentration for 6 (4+6 h sample) or 20 h (4+20 h sample). The 4+20 h samples showed robust enzyme activity for the 4 substrates, while the activities were barely detected in the 4+6 h sample except for LEHD-AMC (see below for the reason why it was ignored) (Fig 7A-D). Importantly, a significant level of cell death (~40% with 40 μM Aβ42) was observed in the 4+6 h samples (Fig 7G). Thus, 4+6 h samples with 40 μM Aβ42 were mainly used for the following PIS and study.

Screening for protease inhibitors which suppress STS- and Aβ42-induced cell death.

Some commercially available inhibitors of serine proteases, caspases and proteasome were employed to analyze their ability to inhibit or reduce the cell death induced by Aβ42 or STS. HeLa cells were treated with 40 μM Aβ42 or 0.5 μM STS with or without this inhibitors for 4+6h and cell viability was assessed by MTT assay. The

results shown that ALLN (calpain inhibitor), MG132 (proteasome inhibitor) and Roscovitine (cdk5 inhibitor) did not show much inhibitory effect against Aβ or STS induced cell death. Leupeptin, a serine protease inhibitor shows equal level of inhibition on STS or Aβ cytotoxicity. The pan caspase inhibitor shows 1.5 fold increase in the survival rate of STS treated cells but not for the Aβ treated cells; in contrast the inhibitor of NS protease Suc-AAPF-CMK shows same level of survival rate in Aβ treated cells. From this PIS data we decided to utilize the Suc-AAPF-CMK to understand the mechanism behind this inhibition on Aβ cytotoxicity.

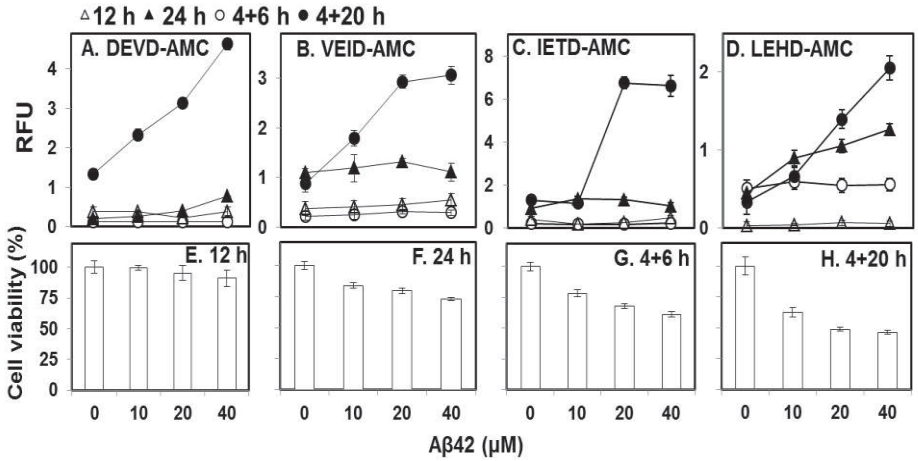

Fig. 7. Effects of Aβ42 on activation of caspases and cell death in HeLa cells (A-D) Cells ($1.5x10^4$) were treated with oligomerized Aβ42 at the indicated concentrations and time. Then, the activities of Caspases -3, -6, -8, -9 of the cell extracts were measured with their respective synthetic substrates (10 μM DEVD-AMC for caspase-3, 50 μM VEID-AMC for caspase-6, 50 μM IETD_AMC for caspase-8, 50 μM LEHD-AMC for caspase-9). (E-H) To check the level of cytotoxicity, cells were plated in 96 well **plates** at 15000 cells per well density and treated with oligomeric Aβ42 at the indicated concentrations and time, cell viability was assessed by MTT assay.

Table. 1. Protease inhibitor screening for identification of inhibitors that suppress cell death induced by STS and Aβ42

Inhibitor	Target	K_i, μM	Conc, μM	STS, fold	Aβ42, fold
z-VAD-fmk	caspase		20	1.5	1.0
Soc-AAPF-cmk	Nuclear scaffold protease	0.0056	40	0.9	1.5
ALLN	calpain	0.19	20	0.9	0.8
MG132	proteasome	0.004	5	1.0	0.7
Leupeptin	serine protease	0.05	20	1.0	1.1
Roscovitine	Cdk5	0.1	10	0.3	0.4

IV-4. Activation of NS protease in Aβ42-induced cell death

The effect of AAPF-CMK identified by PIS method was reexamined on the cell death induced by Aβ42. Cell death was assessed by measurement of reduction of cellular MTT and alamarBlue. Cells treated with 40 μM Aβ42 for 4+6 h as above showed ~40% decrease of the cellular MTT reduction to MTT formazan (Fig 8A). A similar value was obtained in alamarBlue assay, confirming occurrence of cell death at the levels under the condition. Addition of z-VAD-FMK at 20 μM resulted in marginal changes in the cell death induced by Aβ42, while soc-AAPF-CMK at 40 μM significantly reduced the cytotoxicity of Aβ42 (Fig 8A). On the other hand the cell death induced by STS was slightly reduced by 20 μM z-VAD-FMK, but not by 40 μM AAPF-CMK (Fig 8B).

Although AAPF-CMK was employed as NS protease inhibitor in the current study, the protease was not clearly characterized. There is only one report to date identifying the protease which was HtrA1/Prss11 [81]. We keep using the term, NS protease, through the current study and biochemical data obtained here are compared to those of the protease, because of the uncertainty. On the other hand, the chemical is

also known to react with ATP-dependent helicase and proteins containing SAP-domains [82). Thus, it was necessary to know which factors are directly relevant to the effect of AAPF-CMK. For the purpose we initially measured enzymatic activity in Aβ42-treated cells with using AAPF-AMC which is a substrate form of AAPF-CMK. Cells treated with STS and other cell damaging agents were also explored for the enzyme activity. As shown in Fig 8C, significant AAPFase activity was detected only in Aβ42-treated cells. We next measured K_M value of the AAPFase activity using cell extracts derived from Aβ42-treated cells. The value was estimated ~245 μM which is similar with the K_M value (250 μM) of NS protease reported before (figure 2D). Altogether, these data strongly suggest the activation of NS protease in Aβ42-treated cells.

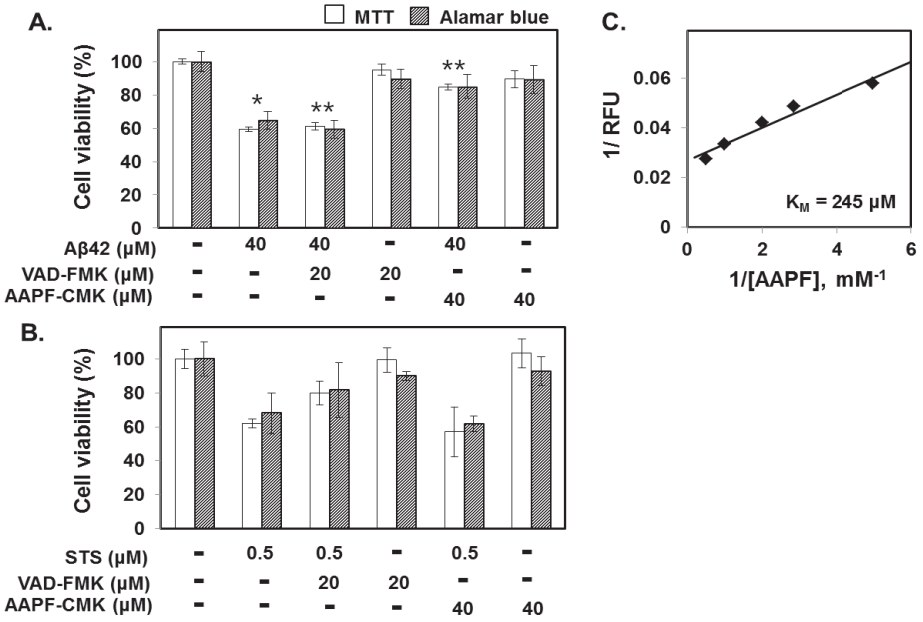

Fig. 8. Effect of z-VAD-FMK and Suc-AAPF-CMK on cell death induced by Aβ42 and STS (A-B) HeLa cells were preincubated with 20 μM z-VAD-FMK or 40 μM Suc-AAPF-CMK for 1h, then the cells were treated with 40 μM oligomeric Aβ42 in the presence or absence of the above mentioned inhibitors for 4+6h. In case of STS, inhibitor pretreated cells were incubated with 0.5 μM STS in the presence or absence of z-VAD-FMK or Suc-AAPF-CMK for 4h. Cell viability was assessed by MTT assay and Alamar blue assay. The error bars represent ± standard deviation. (C) Lineweaver-Burk plot of 1/V versus 1/S for Suc-AAPF-AMC hydrolysis by NS protease activity. Aβ42 treated cell extracts were prepared and assayed for 2h with indicated concentrations of Suc-AAPF-AMC.

IV-5. Differential processing of lamin A/C and B in STS- and Aβ42-treated cells

The activation of NS protease was further explored. One well-known substrate of NS protease is lamin proteins which are also substrates of caspase-6 [83]. Caspases have been revealed to be activated in STS-treated cells [84], while the activity was poor (Fig 7) and instead, NS-protease-like activity (AAPFase) was detected in Aβ42-treated 4+6 h samples (Fig 8). In the following experiments, the processing of lamin proteins was compared in STS- and Aβ42-treated cells using immunoblot assay. Lamin A and its homologous lamin C are 664 and 572 amino acid long, respectively, while lamin B_1 is composed of 586 amino acids. The lamin cleavage by caspase-6 occurs at C-terminus of Asp230 in lamin A/C and D231 in lamin B_1, respectively. On the other hand, NS protease cleaves lamin A/C at Tyr376 and lamin B1 at Tyr376 [85]. Thus, it is possible to determine the enzyme responsible for the cleavage by examining the size of products.

In STS-treated cells cleaved products were detected for lamin A/C (Fig 9A and 9C) and lamin B (Fig 9A) as well as caspase-9, -8, -3, -6, DFF40/45 (substrate of caspase-3). Level of Bid (substrate of

caspase-8) decreased, suggesting it was also processed in the cells (Fig 9A). The results are in well accordance with previous studies indicating activation of caspase-dependent intrinsic apoptotic pathway (ref). In Aβ42-treated 4+6 h samples at all Aβ42 concentrations no processing of caspases and their substrates was detected (Fig 9B), consistent with the results shown in figure 1 except LEHDase activity. LEHD-AMC was employed to assay caspase-9 activity (ref). However, procaspase-3, substrate of active caspase-9, and DFF40/45, substrates of active caspase-3 were barely changed (Fig 9B). Thus, it is questionable if the activity was from caspase-9.

The levels of nuclear lamin A and B were reduced in the 4+6 h samples with high concentrations (30-60 μM) of Aβ42 (Fig 9B). Differences were clearly noticed between the STS and 4+6 h samples. In STS-treated cells, both lamin A and C were diminished (Fig 9A), whereas lamin A levels were reduced but lamin C levels were barely changed in the 4+6 h sample (Fig 9B). Furthermore, a new protein (~46 kDa) which is seemingly a cleaved product of lamin B (ref) was detected clearly in STS-treated cells (Fig 9A), while any other bands related to the protein were undetectable in the 4+6 h samples (Fig 9E). Moreover, faint but substantial protein band estimated ~46 kDa was detected in

lamin A/C immunoblot analysis of the 4+6 h samples (Fig 9D). Instead, ~28 kDa protein bands were observed in the STS-treated cells (Fig 9C). ~28 kDa and ~46 kDa peptides were detected in the STS-treated cells in the immunoblot analysis using antibodies specific for N-terminus of lamin A/C and C-terminus of lamin B_1, respectively (figure 9 and 10). Those peptides are corresponding to the products generated by caspase-6 (ref), indicating involvement of caspase-6 in STS-induced cleavage of lamins.

On the other hand, the reduction of lamin A in Aβ42-treated cells (figure 9B) seems to be due to the catalytic activity of NS protease, for ~46 kDa peptide detected in the immunoblot assay using antibody specific for N-terminus of lamin A/C are corresponding to the peptide generated by cleavage of lamin A (figure 9D). However, lamin C homologous to lamin A was barely reduced in the Aβ42-treated cells (figure 9B and 4). We referred to other publications to explain the preferential cleavage of lamin A to lamin C, but failed to find the similar observations. This observation remains to be explored. The cleavage of lamin B_1 by NS protease was expected to generate ~21 kDa peptide [87] in Aβ42-treated cells, but we failed to detect the peptide in the Aβ42-treated cells even after extensive exposure of the immunoblot to

the detection apparatus. The reduction, however, was diminished in the presence of AAPF-CMK (see below). Thus, we speculated that the reduction of lamin B_1 was due to cleavage by NS protease.

The reduction of lamin A and B was observed in the 4+20 h samples with 20-60 μM of Aβ42 (figure 9F). However, unlike those of 4+6 h samples, activities of caspases with the four different substrates were robust in the 4+20 h samples (figure 7A-D). Accordingly, the processing of caspases were detected in the sample on the immunoblot assay (figure 9C). Levels of procaspase-9 decreased in an Aβ42-dose dependent manner. Cleaved caspase-8 was also seen (figure 9F), although it is questionable if the cleaved product of caspase-8 is catalytically active, because cleavage of Bid was not detected. Procaspase-3 and its substrate, DFF40/45 was partially processed in the same sample treated with higher concentrations (30~60 μM) of Aβ42 (figure 9F). The reduction pattern of the lamin proteins in the 4+20 h samples, however, was different from that of STS-treated cells. It was rather similar to that of the 4+6 h sample. Thus, it is likely that the reduction of lamin A and B in the 4+20 h samples was caused by NS protease rather than the active caspases. It might be because lamin cleaving caspase would not be sufficiently active, as processing of

procaspase-6 was not detected in the 4+20 h samples.

No reduction of lamin A and B was detected in 24 h samples (figure 9G). Furthermore, no processing of the caspases and their substrates was detected in the sample (figure 9G), which was unexpected because significant levels of activities were detected in the assay with synthetic substrates (figure 7). The discrepancy may be due to differential sensitivity between the two assay methods. Although detection of cleaved product of caspases and their substrates by the western immunoblot assay is a method to demonstrate the activation clearly, enzyme activity assay is often more sensitive. Thus, we think that weak activation occurred in 24 h sample. The activity with LEHD-AMC was higher in the 24 h samples than in 4+6 h sample. This strongly suggests that the activity is not related with the reduction lamin A and C.

The time point for the double treatment employed in the previous experiments was determined in cells double-treated with Aβ42 initially for 1, 2, and 4 h and then for 2, 4, 6 and 8 h. 40 μM Aβ42 was used in the present and following experiments, because the reduction was clearly seen in samples with the concentration of Aβ42. The reduction of lamin A (and similarly lamin B) was prominently observed in

2+8, 4+4, 4+6 and 4+8 h samples (figure 10A). We chose 4+6 h for the present study because it is a mid-point. The effect of other Aβ42 structural species on the reduction was also explored. Fibrillar Aβ42 peptide showed barely the effect, while monomeric peptide at 40 μM induced the reduction of lamin A and B (figure 10B). The monomeric preparation, however, often produced less cell death and fibrillar preparation was not effective in inducing cell death (data not shown), compared to the oligomeric preparation (ref). Thus, oligomeric preparation of Aβ42 was preferentially used throughout the current study.

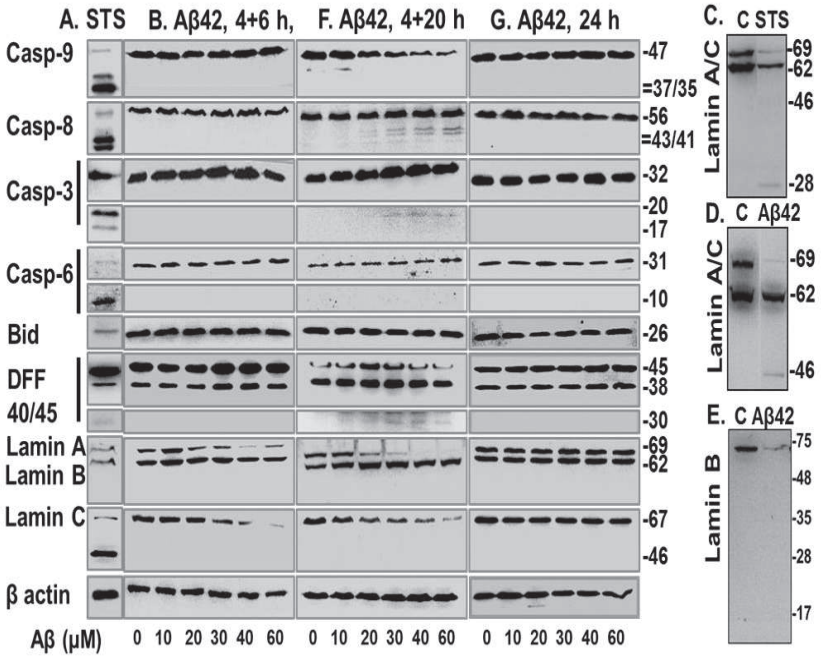

Fig. 9. Effect of Aβ42 and STS on Caspases and its substrate processing: Immunoblot analysis of caspase and its substrates. HeLa cells were incubated with Aβ42 at the indicated concentrations and time points or with 0.5 μM STS for 6h. Total Cell extracts were prepared and assessed for processing of caspase-3, -6, -8, -9 and its substrates Bid, DFF40/45, Lamin A/C and Lamin B by western blotting. (A) STS induced caspases and its substrate processing. (B) Concentration dependent cleavage of lamin A and B observed in 4+6h treated cells but processing of caspases and its substrates were not observed. (C-E) STS and Aβ42 treated cell extracts shows differential cleavage of Lamin A/C and B. (F) western blot images of caspase processing in 4+20 and 24h Aβ42 treated HeLa cell extracts. Actin was employed as a loading control. The relative molecular weights (in kDa) were indicated at the left.

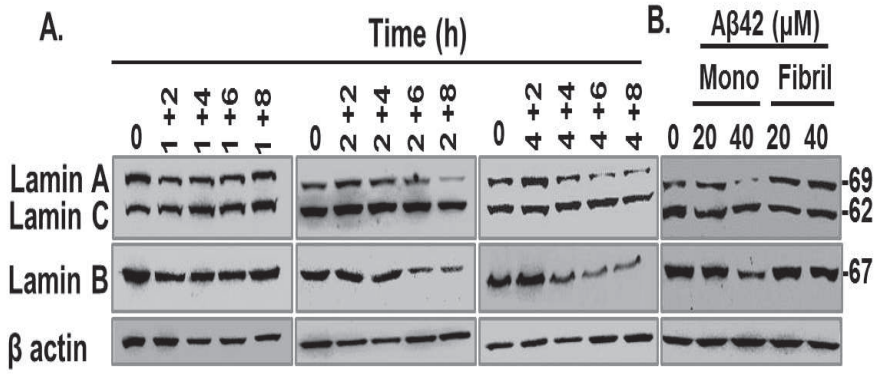

Fig. 10. Time and Species dependent cleavage of Lamin A and B by Aβ42 (A) HeLa cells ($4x10^5$) were treated with 40 μM Aβ42 for the indicated time periods, total cell lysate were prepared and analyzed for the processing of Lamin A/C and B by immunoblot. (B) HeLa cells ($4x10^5$) were incubated with 20 and 40 μM concentrations of monomeric and fibrillar Aβ42 for 4+6 h and cell extracts were immunoblotted for Lamin A/C and B. Actin was employed as a loading control. The relative molecular weights (in kDa) were indicated at the left.

IV-6. NS protease inhibitor but not caspase inhibitor reduces Aβ42-induced lamin A and B cleavage

STS-induced reduction of lamin A/C and production of ~46 kDa product from lamin B were significant inhibited by 20 μM z-VAD-FMK, Aβ42-induced reduction of the proteins was barely affected by the inhibitor at up to 100 μM of z-VAD-FMK (only 20 μM data is shown in figure 11A). Conversely, the Aβ42-induced reduction of lamin A and B was diminished in the presence of AAPF-CMK which was not effective in STS-induced reduction of lamin A and B (figure 11B). These data indicate involvement of NS protease in Aβ42-treated 4+6 h sample and caspase in STS-treated cells, again confirming the different nature of the lamin reduction in the two cell death types. We use the concentration of AAPF-CMK in the following experiments, because higher concentration of the inhibitor caused cell death for itself and lower concentration was not as effective as the concentration (data not shown). Other selected protease inhibitors such as ALLN (calpain inhibitor), MG132 (proteasome inhibitor), EDTA (metalloprotease inhibitor) and leupeptin (serine protease inhibitor) were not effective in the reduction of lamin proteins (figure 11C), excluding the participation of those proteases in

the process.

We also examined if Cdk5 deregulation functions in the reduction, because the deregulation of the kinase triggers nuclear lamina dispersion and cell death before caspase activation (ref). Inclusion of 10 μM roscovitine a strong and specific inhibitor of Cdk5, barely affected the reduction of the proteins induced by Aβ42 in 4+6 h sample (figure 11D), unlikely that Cdk5 deregulation plays an essential role in the reduction of lamin proteins.

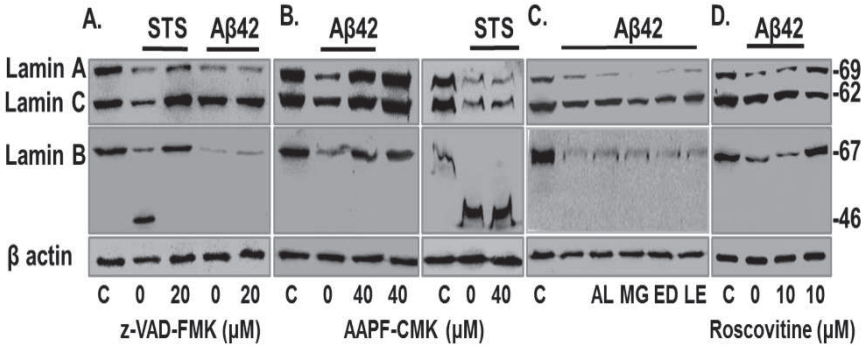

Fig. 11. NS protease inhibitor but not caspase inhibitor reduces Aβ42-induced lamin A and B cleavage (A-B) HeLa cells were exposed to indicated concentrations of z-VAD-FMK and AAPF-CMK for 1h prior to Aβ treatment and incubated with 40 μM Aβ42 or 0.5 μM STS in the presence or absence of z-VAD-FMK or Suc-AAPF-CMK for 4+6h. Cell extracts were prepared and analyzed for Lamin A/C and B processing. (C) HeLa cells were incubated with 40 μM Aβ42 in the presence of ALLN (AL) calpain inhibitor, MG132 (MG) proteasome inhibitor, EDTA (ED) metallopeptidase inhibitor and leupeptin (LE) serine protease inhibitor and immunoblotted for Lamin A/C and B. (D) HeLa cells were incubated with 40 μM Aβ42 with or without cdk5 inhibitor roscovitine for 4+6h and immunoblotted for Lamin A/C and Lamin B.

IV-7. Aβ42 induces nuclear deformation which is suppressed by NS protease inhibitor

Alteration in levels of lamin A/C and B proteins likely causes nuclear abnormalities. Thus, we subsequently analyzed nuclear integrity of the 4+6 h sample with 40 μM Aβ42 using Hoechst staining and immunofluorescence microscopy for lamin A/C and B. Nuclear deformation as shown in the images of representative cells was observed with high frequency in the sample (Hoechst stained samples of figure 12). Changes in the lamin epitope detected by lamin A/C and B antibodies were also observed accordingly to the nuclear deformation (figure 12). The deformation is morphologically similar to those observed in primary fibroblast with lamin A/C mutation [87] or induced by Simian virus 40 [88]. On the other hand, condensation of nuclei seen in STS-induced cells were rarely seen in the 4+6 h sample (figure 12), further demonstrating the involvement of different mechanism in the two cell death processes. Nuclear envelope dispersion reported previously for Aβ-treated HT22 cells [89] was rarely observed in the sample.

We next asked if NS protease and caspase were involved in the nuclear deformation observed in the 4+6 h sample. The nuclear deformation and

changes in the levels of the lamin A/C and B epitopes were significantly diminished in sample prepared with 40 μM AAPF-CMK as shown in the images of representative cells (figure 12), whereas z-VAD-FMK at 20 μM was not so effective in suppression of the changes in nucleus. These results indicate that the nuclear deformations induced by Aβ42 are due to NS protease-dependent but caspase-independent process. Cdk5 played a minimal role in Aβ42-induced nuclear deformation, as the inhibitor of the kinase, roscovitine, has little effect on the deformation (figure 12).

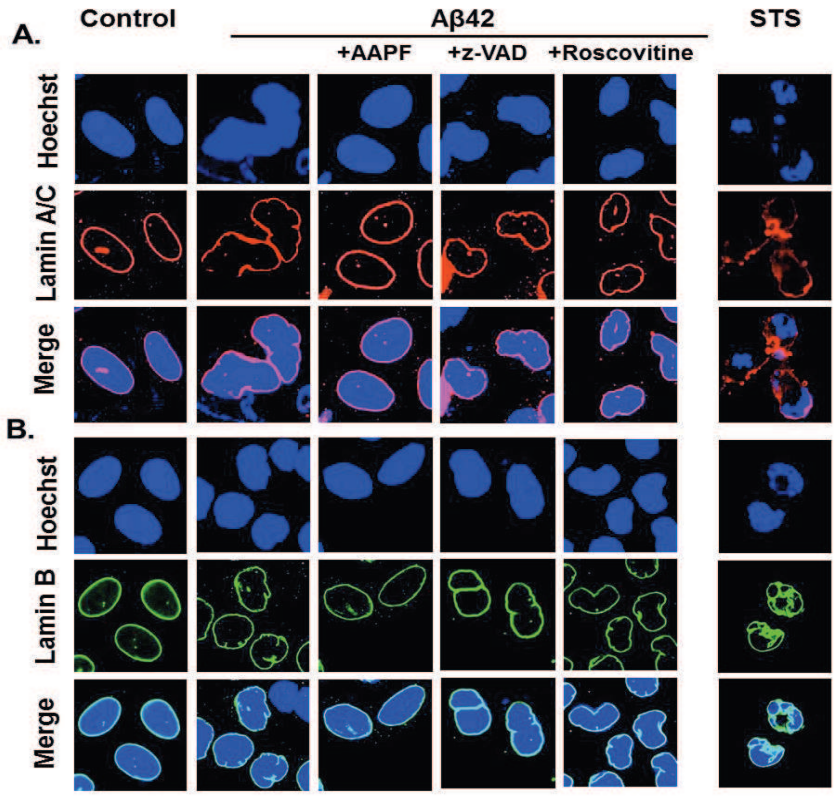

Fig. 12. Aβ42 induces nuclear deformation which is suppressed by NS protease inhibitor (A) Confocal image analysis of HeLa cells treated with Aβ42 in the presence or absence of caspase (z-VAD-FMK), NS protease (Suc-AAPF-CMK), Roscovitine (Cdk5) inhibitors. Cells were treated with 0.5 μM STS and nuclear deformation also observed. Primary goat anti-lamin A/C and Lamin B in addition to secondary anti-goat IgG-FITC and anti-goat IgG-Rhodamine antibodies were used to detect lamin A/C (Red) and lamin B (green). Nuclei were seen with the Hoechst staining. Images were visualized using a confocal microscope (LSM510, Carl Zeiss).

IV-8. DISCUSSION

Nuclear envelope is supported by the nuclear scaffold composed of both structural and functional proteins. Polymerization of the intermediated filament proteins, nuclear lamin A and B, generates the nuclear lamina, the major structural components of the nuclear scaffold. The lamins are also essential for many nuclear functions such as chromatin organization, DNA replication, transcription, and DNA repair (reviewed in genes develop 2008 22:832).

Modifications of the nuclear lamin proteins are common processes in dying cells. Nuclear deformation and dispersion and fragmentation of the nuclear envelope observed in the cells have been revealed as results of the modification [88-89]. One example of those modifications occurring in Aβ-treated cells is CDK5-mediated phosphorylation of lamin A and B which resulted in the nuclear dispersion [89]. In the current study, however, rather than the nuclear dispersion the reduction of lamin A and B (figures 9) and deformation of the nuclear lamina (figures 12) were recognized in the Aβ-treated cells. Furthermore, the lamin reduction and the lamina deformation were independent on the activity of CDK5, as revealed by the observation

that the processes were resistant to Cdk5 inhibitor Roscovitine (figure 11 and 12). The reason for the discrepancy requires further investigation, but one potential explanation for it might be the different experimental conditions. In the current study 42 amino acid-long Aβ oligomerized as indicated were employed (figure 7), while short Aβ (25-35) was used in the previous study (ref). It has been revealed that even the same sized peptides resulted in different biological consequences, if their conformations are different (eg. oligomer vs. fibrils) (see figure 10 as an example). Furthermore, in the current study cells were treated twice with Aβ42 to attain the condition shown in figure 7. As shown in figure 9, single treatment of cells with the same Aβ42 preparation resulted in the different consequences.

Proteolytic degradation of lamins is other major modification responsible for the nuclear deformation and fragmentation. At least two enzymes have been known to catalyze the cleavage of lamins. One of those proteases is caspase-6 which is an executioner caspase activated by the upstream caspases such as caspase-3 during apoptosis [90].

Although the lamin cleavage by caspase-6 is clearly late process occurring after activation of apoptotic cell death pathway, the cleavage by NS protease can be an early process preceding other cell

death processes, as illustrated in glutamate-induced cerebellar granule cell apoptosis in which the lamin cleavage and dissolution of the microtubule network preceded chromatin fragmentation (Ankarcrona *et al.*, 1996 Neuroreport 7, 2659–2664). Other example of process preceding apoptosis is the nuclear dispersion induced by phosphorylation of lamin A and B by CDK5 which was suggested to be an early and irreversible trigger for cell death in Aβ-treated cells [89]. In the current study, we also show that Aβ resulted in nuclear deformation and reduction of lamin proteins before activation of caspase. Furthermore, it is shown that the two processes occurred independently of caspase activity (figure 11 and 12). The cell death induced by Aβ was significantly reduced by AAPF-CMK, but not by VAD-FMK, suggesting the importance of NS protease in the cell death rather than in the caspase-dependent apoptosis. Interestingly, the lamins were cleaved by NS protease rather than caspase even in cells in which caspases were activated as shown in Aβ-treated 4+20 h sample (figure 9F). In the cells, caspase-6 activation was not detected (figure 9F), although caspase-6-like VEIDase activity was seen (figure 7B). It remains to explore whether the low activity of caspase-6 or other unknown factors might result in the caspase-independent cleavage of lamins.

In conclusion, we show that lamin A and B reduction and consequent nuclear morphological change occur in cells treated by Aβ42 before caspase activation. Data of our study indicate that the reduction of lamin proteins may be due to NS protease function. Suppression of NS protease by its inhibitor, AAPF-CMK, effectively inhibited the cell death induced by Aβ42. This study provides an idea that inhibition of NS protease might be an effective way to control pathological process of AD.

V. FUTURE RESEARCH

V-1. INTRODUCTION

Several studies have reported that amyloid beta can induce caspase activation in cultured cells. But the interaction between amyloid beta and caspases were poorly studied. Previous work from our group demonstrated that Aβ42 can directly bind and inhibits the activity of procaspase-9 and apoptosome formation in HeLa cells (data not shown). To confirm these effects on other caspases, we carried out an experiment by incubating different concentrations of amyloid beta 42 with various forms of purified recombinant caspases and analyzed the activity.

V-2. MATERIALS AND METHODS

V-2.1. Production of recombinant caspases

Recombinant caspases were purified as described previously (109, 111). Briefly, Procaspase-4 (mutant at E93A, D104A, D270A, D289A), Procaspase-6 (mutant at D23A, D193A, D179A), Procaspase-7 (C186S), active caspases -2, -4, -6, -7, -8, (wild type), and caspase -2,

-4, -7 lacking prodomain (Δp), cloned in pET28 vector were over expressed in pLysS *E.Coli* strain. The caspases were purified by two successive chromatographic procedures. Initially, bacterial cell lysates prepares by sonication and centrifugation at 2000 rpm for 1h in buffer contain 20mM Tris-HCL, pH 8.0,, 10 mM NaCl, 0.1 mM EDTA, 0.1 mM PMSF, 1 mM β-mercaptoethanol. The supernatant was loaded onto a Ni-NTA column (Qiagen) pre equilibrate with buffer contain 20 mM Tris-HCL, pH 8.0, 10 mM NaCl, 1 mM β-mercaptoethanol, 10% glycerol and eluted with same buffer supplemented with 250 mM imidazole. The active fractions were diluted and applied to a HiTrapQ Sepharose column (Amersham Pharmacia Biotech) equilibrated with buffer contain 20 mM HEPES-NaOH, pH 7.5, 10 mM NaCl, 0.1 mM EDTA, 1 mM DTT, 10% glycerol and eluted with 1-400 mM NaCl gradient. The purified proteins were dialyzed against 20 mM HEPES (pH 7.5), 10 mM NaCl, 1 mM EDTA, 2 mM DTT and 10% glycerol; the aliquots were saved at -80 ^{o}C before use.

V-2.2. Measurement of purified caspase activity using synthetic substrates

The activities of purified Procaspase-2, ΔP caspase -2,

Procaspase-4, caspase-4, ΔP caspase -4, Procaspase-6, caspase-6, procaspase-7, capase-7, ΔP caspase -7 and caspase-8 were measured in the presence or absence of indicated amount of Aβ42 in caspase assay buffer (pH 7.0) using VDVAD-AMC (50 μM), YVAD-AMC (50 μM), VEID-AMC (50 μM), DEVD-AMC (10 μM), IETD-AMC (50 μM) respectively. The fluorescence of the AMC release from the substrates was measured as described above.

V-2.3. Immunocytochemistry

HeLa cells were seeded in 12 well plate at 70% confluency, cultured for 24h and further incubated for 12h in serum free media and then treated with 20 μM Aβ42. After treatment, cells were fixed in methanol at -20 ^{o}C and permeabilized by 0.3% Triton X-100. After blocking with 0.1% BSA overnight, mouse anti amyloid beta (6E10) and rabbit anti caspase-2, goat anti caspase-4, -6, -7 and -8 were added to each samples and incubated at 4°C overnight. After washing with PBS, Alexa-Fluor-543 conjugated secondary antibodies for caspase and Alexa-Flour-488 conjugated chicken anti-mouse IgG antibodies for Aβ42 (dilution, 1:200) were treated for 2h at room temperature followed by PBS washing. Nuclei were stained with Hoechst and confocal images

were obtained with Carl Zeiss LSM510 microscope (Jena, Germany) using vendor provided software (LSM 510).

V-3. RESULTS AND DISCUSSION

The results shown, enzymatic activity of processed caspase 4 and 6 were inhibited by Aβ42. The inhibition was in a dose dependent manner for caspase 4 but in case of caspase 6, 50% of inhibition was observed even at 2uM concentration and saturated up to 40uM. Aβ42 barely inhibited the activity of procaspase 4 but not procaspase 6. Activity of procaspase 2, **Δ**p caspase 2, procaspase 7, Processed caspase 7, **Δ**p caspase 7 and processed caspase 8 was not affected by Aβ42 (Fig. 13).

The confocal images show the internalization and interaction of Aβ42 with caspase 6, but interaction with other caspases was not identified (Fig. 14). These observations from both enzyme assays and confocal imaging support the direct interaction of amyloid beta with caspase-6. But still it has to be investigated in more detail to understand the mechanism, which may give some new concepts on Aβ induced cytotoxicity.

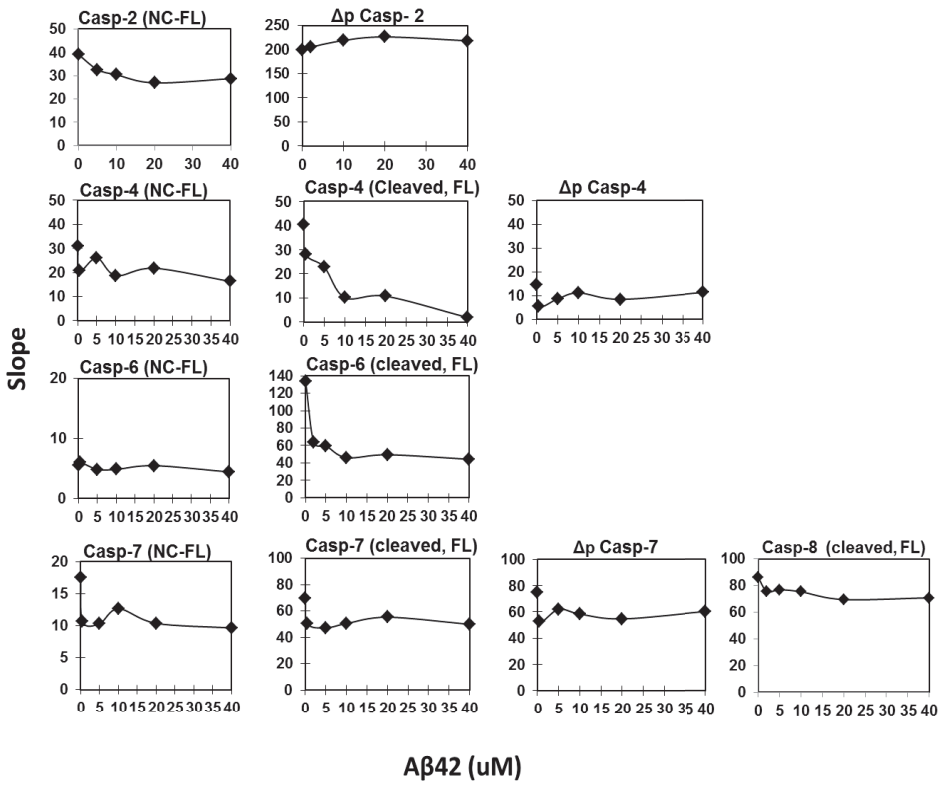

Fig. 13. Effect of Aβ42 on purified recombinant Caspases activity: Purified recombinant caspases were incubated with indicated concentrations of Aβ42 and their activity was measured with their respective synthetic substrates for 1h and the release of AMC was monitored for 1h in 1 minute interval at excitation and emission wavelengths of 360 nm and 480 nm respectively, using microplate spectrofluorometer (Molecular Devices, CA, USA). The results were expressed as a slope of total readings versus Aβ42 concentration.

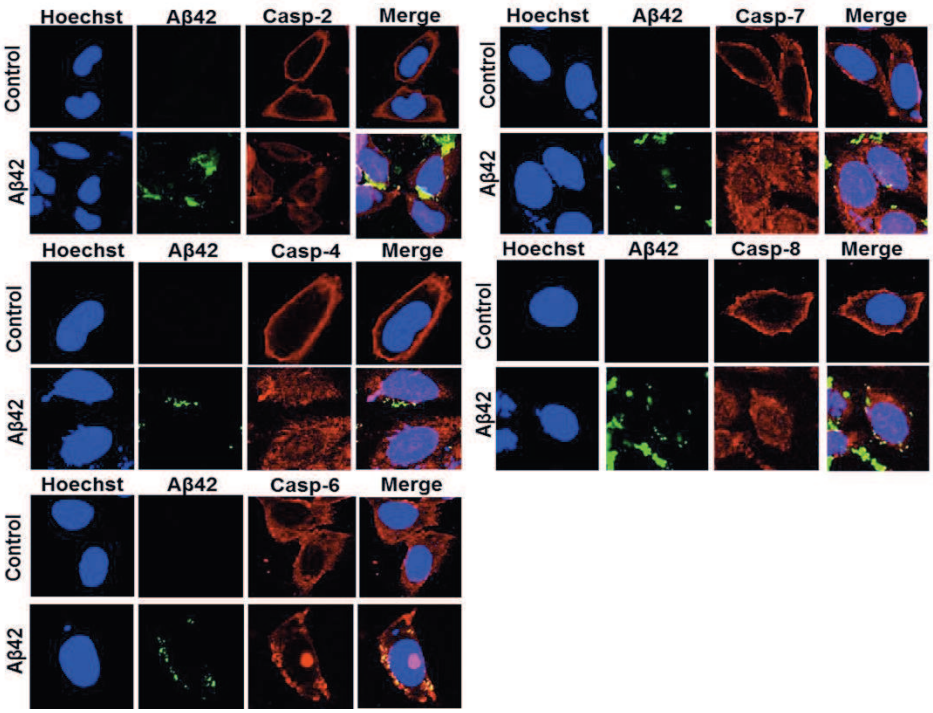

Fig. 14. Aβ42 binds Caspase-6 but not with Caspase -2, -4, -7 and -8

(A-E) HeLa cells were cultured and treated with 20 μM Aβ42 for 12h. Cells were fixed and permeabilized by methanol and triton x-100. Primary mouse anti amyloid beta (6E10) and rabbit anti caspase-2, goat anti caspase-4, -6, -7 and -8 antibodies in addition to secondary anti-mouse IgG-FITC and anti-rabbit or anti-goat IgG rhodamine antibodies were used to detect intracellular Aβ (green) and caspases (red). Nuclei were seen with the nucleic acid flurochrome Hoechst and images were visualized using a confocal microscope.(LSM 510, Carl Zeiss).

VI. REFERENCES

1. D. J. Selkoe, Alzheimer's disease: genotypes, phenotypes, and treatments, Science 275 (1997) 630-631.

2. D. J. Selkoe, Alzheimer's disease: genes, proteins, and therapy, Physiol Rev 81 (2001) 741-766.

3. R. D. Terry, N. K. Gonatas, and M. Weiss, The ultrastructure of the cerebral cortex in Alzheimer's disease, Trans Am Neurol Assoc 89 (1964) 12.

4. Goate, M. C. Chartier-Harlin, M. Mullan, J. Brown, F. Crawford, L. Fidani, L. Giuffra, A. Haynes, N. Irving, L. James, and et al., Segregation of a missense mutation in the amyloid precursor protein gene with familial Alzheimer's disease, Nature 349 (1991) 704-706.

5. Y. H. Suh, An etiological role of amyloidogenic carboxyl-terminal fragments of the beta-amyloid precursor protein in Alzheimer's disease, J Neurochem 68 (1997) 1781-1791.

6. Y. H. Suh, and F. Checler, Amyloid precursor protein, presenilins, and alpha-synuclein: molecular pathogenesis and pharmacological applications in Alzheimer's disease, Pharmacol Rev 54 (2002) 469-525.

7. L. Lannfelt, Genetics of Alzheimer's disease, Acta Neurol Scand Suppl 168 (1996) 25-27.

8. M. Shoji, T. E. Golde, J. Ghiso, T. T. Cheung, S. Estus, L. M. Shaffer, X. D. Cai, D. M. McKay, R. Tintner, B. Frangione, and et al., Production of the Alzheimer amyloid beta protein by normal proteolytic processing, Science 258 (1992) 126-129.

9. J. T. Jarrett, E. P. Berger, and P. T. Lansbury, Jr., The carboxy terminus of the beta amyloid protein is critical for the seeding of amyloid formation: implications for the pathogenesis of Alzheimer's disease, Biochemistry 32 (1993) 4693-4697.

10. J. A. Hardy, and G. A. Higgins, Alzheimer's disease: the amyloid cascade hypothesis, Science 256 (1992) 184-185.

11. J. Hardy, and D. J. Selkoe, The amyloid hypothesis of Alzheimer's disease: progress and problems on the road to therapeutics, Science 297 (2002) 353-356.

12. D. Burdick, B. Soreghan, M. Kwon, J. Kosmoski, M. Knauer, A. Henschen, J. Yates, C. Cotman, and C. Glabe, Assembly and aggregation properties of synthetic Alzheimer's A4/beta amyloid peptide analogs, J. Biol. Chem. 267 (1992) 546-554.

13. C. J. Pike, A. J. Walencewicz, C. G. Glabe, and C. W. Cotman, In vitro aging of beta-amyloid protein causes peptide aggregation and neurotoxicity, Brain Res 563 (1991) 311-314.

14. J. Busciglio, A. Lorenzo, and B. A. Yankner, Methodological variables in the assessment of beta amyloid neurotoxicity, Neurobiol Aging 13 (1992) 609-612.

15. C. Geula, C. K. Wu, D. Saroff, A. Lorenzo, M. Yuan, and B. A. Yankner, Aging renders the brain vulnerable to amyloid beta-protein neurotoxicity, Nat Med 4 (1998) 827-831.

16. C. A. McLean, R. A. Cherny, F. W. Fraser, S. J. Fuller, M. J. Smith, K. Beyreuther, A. I. Bush, and C. L. Masters, Soluble pool

of Abeta amyloid as a determinant of severity of neurodegeneration in Alzheimer's disease, Ann Neurol 46 (1999) 860-866.

17. J. Wang, D. W. Dickson, J. Q. Trojanowski, and V. M. Lee, The levels of soluble versus insoluble brain Abeta distinguish Alzheimer's disease from normal and pathologic aging, Exp Neurol 158 (1999) 328-337.

18. J. P. Cleary, D. M. Walsh, J. J. Hofmeister, G. M. Shankar, M. A. Kuskowski, D. J. Selkoe, and K. H. Ashe, Natural oligomers of the amyloid-beta protein specifically disrupt cognitive function, Nat Neurosci 8 (2005) 79-84.

19. M. P. Lambert, A. K. Barlow, B. A. Chromy, C. Edwards, R. Freed, M. Liosatos, T. E. Morgan, I. Rozovsky, B. Trommer, K. L. Viola, P. Wals, C. Zhang, C. E. Finch, G. A. Krafft, and W. L. Klein, Diffusible, nonfibrillar ligands derived from Abeta1-42 are potent central nervous system neurotoxins, Proc Natl Acad Sci U S A 95 (1998) 6448-6453.

20. P. N. Lacor, M. C. Buniel, L. Chang, S. J. Fernandez, Y. Gong, K. L. Viola, M. P. Lambert, P. T. Velasco, E. H. Bigio, C. E. Finch, G.

A. Krafft, and W. L. Klein, Synaptic targeting by Alzheimer's-related amyloid beta oligomers, J Neurosci 24 (2004) 10191-10200.

21. Snyder EM, Nong Y, Almeida CG, Paul S, Moran T, Choi EY, NairnAC, SalterMW, Lombroso PJ, Gouras GK, Greengard P (2005) Regulation of NMDA receptor trafficking by amyloid-beta. Nat Neurosci 8, 1051-1058.

22. Yamamoto N, Matsubara E, Maeda S, Minagawa H,Takashima A, Maruyama W, Michikawa M, Yanagisawa K (2007) A ganglioside-induced toxic soluble Abeta assembly.Its enhanced formation from Abeta bearing the Arctic mutation. *J Biol Chem* **282**, 2646-2655.

23. Hansma HG, Laney DE, Bezanilla M, Sinsheimer RL, Hansma PK (1995) Applications for atomic force microscopy of DNA. *Biophys J* **68**, 1672-1677.

24. Rabizadeh S, Bitler CM, Butcher LL, Bredesen DE (1994) Expression of the low-affinity nerve growth factor receptor enhances beta-amyloid peptide toxicity. *Proc Natl Acad Sci U S A* **91**, 10703-10706.

25. Yaar M, Zhai S, Pilch PF, Doyle SM, Eisenhauer PB, Fine RE, Gilchrest BA (1997) Binding of beta-amyloid to the p75 neurotrophin receptor induces apoptosis. A possible mechanism for Alzheimer's disease. *J Clin Invest* **100**, 2333-2340.

26. Perini G, Della-Bianca V, Politi V, Della Valle G, Dal-Pra I,Rossi F, ArmatoU(2002) Role of p75 neurotrophin receptor in the neurotoxicity by beta-amyloid peptides and synergistic effect of inflammatory cytokines. *J Exp Med* **195**,907-918.

27. Yamin G (2009)NMDA receptor-dependent signaling pathways that underlie amyloid beta-protein disruption of LTP in the hippocampus. *J Neurosci Res* **87**, 1729-1736.

28. Zhao D,Watson JB, Xie CW (2004) Amyloid beta prevents activation of calcium/calmodulin-dependent protein kinase II and AMPA receptor phosphorylation during hippocampal long-term potentiation. *J Neurophysiol* **92**, 2853-2858.

29. De Felice FG, Velasco PT, Lambert MP, Viola K, Fernandez SJ, Ferreira ST, Klein WL (2007) Abeta oligomers induce neuronal oxidative stress through an N-methyl-D-aspartate receptor-

dependent mechanism that is blocked by the Alzheimer drug memantine. *J Biol Chem* **282**, 11590-11601.

30. Moolman DL, Vitolo OV, Vonsattel JP, Shelanski ML (2004) Dendrite and dendritic spine alterations in Alzheimer models. *J Neurocytol* **33**, 377-387.

31. Oddo S, Caccamo A, Shepherd JD, Murphy MP, Golde TE, Kayed R, Metherate R, Mattson MP, Akbari Y, LaFerla FM (2003) Triple-transgenic model of Alzheimer's diseasewith plaques and tangles: Intracellular Abeta and synaptic dysfunction. *Neuron* **39**, 409-421.

32. Spires TL, Meyer-Luehmann M, Stern EA, McLean PJ,Skoch J, Nguyen PT, Bacskai BJ, Hyman BT (2005) Dendritic spine abnormalities in amyloid precursor protein transgenic mice demonstrated by gene transfer and intravital multiphoton microscopy. *J Neurosci* **25**, 7278-7287.

33. Xu H, Greengard P, Gandy S (1995) Regulated formation of Golgi secretory vesicles containing Alzheimer beta-amyloid precursor protein. *J Biol Chem* **270**, 23243-23245.

34. Mizuguchi M, Ikeda K, Kim SU (1992) Differential distribution of cellular forms of beta-amyloid precursor protein in murine glial cell cultures. *Brain Res* **584**, 219-225.

35. Almeida CG, Takahashi RH, Gouras GK (2006) Betaamyloid accumulation impairs multivesicular body sorting by inhibiting the ubiquitin-proteasome system. *J Neurosci* **26**, 4277-4288.

36. Chyung JH, Raper DM, Selkoe DJ (2005) Gamma-secretase exists on the plasma membrane as an intact complex that accepts substrates and effects intramembrane cleavage. *J Biol Chem* **280**, 4383-4392.

37. Xu H, Greengard P, Gandy S (1995) Regulated formation of Golgi secretory vesicles containing Alzheimer beta-amyloid precursor protein. J Biol Chem 270, 23243-23245.

38. Oddo S, Caccamo A, Green KN, Liang K, Tran L, Chen

39. Y, Leslie FM, LaFerla FM (2005) Chronic nicotine administration exacerbates tau pathology in a transgenic model of Alzheimer's disease. *Proc Natl Acad Sci U S A* **102**,3046-3051.

40. Bu G, Cam J, Zerbinatti C (2006) LRP in amyloid-beta production and metabolism. *Ann N Y Acad Sci* **1086**,35-53.

41. Deane R, DuYan S, Submamaryan RK, LaRue B, Jovanovic S, Hogg E,Welch D, Manness L, Lin C,Yu J, Zhu H, Ghiso J, Frangione B, Stern A, Schmidt AM, Armstrong DL, Arnold B, Liliensiek B, Nawroth P, Hofman F, Kindy M, Stern D, Zlokovic B (2003) RAGE mediates amyloid-beta peptide transport across the blood-brain barrier and accumulation in brain. *Nat Med* **9**, 907-913.

42. Almeida CG, Takahashi RH, Gouras GK (2006) Betaamyloid accumulation impairs multivesicular body sorting by inhibiting the ubiquitin-proteasome system. *J Neurosci* **26**, 4277-4288.

43. Wogulis M, Wright S, Cunningham D, Chilcote T, Powell K, Rydel RE (2005) Nucleation-dependent polymerization is an essential component of amyloid-mediated neuronal cell death. *J Neurosci* **25**, 1071-1080.

44. Jin Wang and Michael J. Lenardo (2000) Roles of caspases in apoptosis, development, and cytokine maturation revealed by

homozygous gene deficiencies. *Journal of cell science* 113,753-757.

45. Junichi hitomi et al., (2004) Involvement of caspase-4 in endoplasmic reticulum stress-induced apoptosis and Aβ-induced cell death. *Journal of cell biology* 165(3) 347-356.

46. L Vande Walle, M Lamkanfi and P Vandenabeele (2008) The mitochondrial serine protease HtrA2/Omi: an overview. Cell death and differentiation 15, 453 – 460.

47. Raynaud F, Marcilhac A. (2006) Implication of calpain in neuronal apoptosis. A possible regulation of Alzheimer's disease. FEBS journal 273 (15):3437-43.

48. Boya P, Kroemer G. (2008) Lysosomal membrane permeabilization in cell death. Oncogene 27(50):6434-51.

49. Gil-Parrado S, Fernández-Montalván A, Assfalg-Machleidt I, Popp O, Bestvater F, Holloschi A, Knoch TA, Auerswald EA, Welsh K, Reed JC, Fritz H, Fuentes-Prior P, Spiess E, Salvesen GS, Machleidt W. (2002) Ionomycin-activated calpain triggers

apoptosis. A probable role for Bcl-2 family members. 277(30):27217-26.

50. N. Rogers, S. Paine, L. Bedford, R. Layfield (2010) Review: The ubiquitin-proteasome system: contributions to cell death or survival in neurodegeneration 36,113-124.

51. Mannello F, Luchetti F, Falcieri E, Papa S. (2005) Multiple roles of matrix metalloproteinases during apoptosis. Apoptosis 10(1):19-24.

52. Ivins KJ, Thornton PL, Rohn TT, Cotman CW. (1999) Neuronal apoptosis induced by beta-amyloid is mediated by caspase-8. Neurobiol Dis. 1999 Oct;6(5):440-9.

53. Kim HE, Du F, Fang M, Wang X. (2005) Formation of apoptosome is initiated by cytochrome c-induced dATP hydrolysis and subsequent nucleotide exchange on Apaf-1. Proc Natl Acad Sci U S A. 2005 Dec 6;102(49):17545-50

54. Lavrik, A Krueger, Schmitz, S Baumann, H Weyd, P H Krammer and S Kirchhoff (2003) The active caspase-8

heterotetramer is formed at the CD95 DISC. Cell Death and Differentiation (2003) 10, 144–145.

55. Morita-Fujimura Y, Fujimura M, Kawase M, Chen SF, Chan PH.(1999) Release of mitochondrial cytochrome c and DNA fragmentation after cold injury-induced brain trauma in mice: possible role in neuronal apoptosis. Neurosci Lett. 1999 Jun 4;267(3):201-5.

56. D Burdick, B Soreghan, M Kwon, J Kosmoski, M Knauer, A Henschen, J Yates, C Cotman and C Glabe (1992) Assembly and aggregation properties of synthetic Alzheimer's A4/beta amyloid peptide analogs. The Journal of Biological Chemistry, 267, 546-554.

57. Goldsbury CS, Cooper GJ, Goldie KN, Müller SA, Saafi EL, Gruijters WT, Misur MP, Engel A, Aebi U, Kistler J.(1997) Polymorphic fibrillar assembly of human amylin. J Struct Biol. 1997 Jun;119(1):17-27.

58. Hyde C, Johnson T, Owen D, Quibell M, Sheppard RC.(1994) Some 'difficult sequences' made easy. A study of interchain

association in solid-phase peptide synthesis. Int J Pept Protein Res. 43(5):431-40.

59. Dobeli, H., Draeger, N., Huber, G., Jakob, P., Schmidt, D., Seilheimer, B., Stuber, D., Wipf, B., and Zulauf, M. 1995. A biotechnological method provides access to aggregation competent monomeric Alzheimer's 1–42 residue amyloid peptide. Biotechnology (N.Y.) 13**:** 988–993.

60. Thapa A, Shahnawaz M, Karki P, Raj Dahal G, Sharoar MG, Yub Shin S, Sup Lee J, Cho B, Park IS.(2008) Purification of inclusion body-forming peptides and proteins in soluble form by fusion to Escherichia coli thermostable proteins. Biotechniques. 2008 May;44(6):787-96.

61. Finder VH, Vodopivec I, Nitsch RM, Glockshuber R. (2010) The recombinant amyloid-beta peptide Abeta1-42 aggregates faster and is more neurotoxic than synthetic Abeta1-42. J Mol Biol. 2010 Feb 12;396(1):9-18

62. R. B. Kapust and D. S. Waugh (1999) Escherichia coli maltose-binding protein is uncommonly effective at promoting the

solubility of polypeptides to which it is fused. Protein Sci. 1999 August; 8(8): 1668–1674.

63. Kellyann D. Pryor, Barbara Leiting (1997) High-Level Expression of Soluble Protein inEscherichia coliUsing a His6-Tag and Maltose-Binding-Protein Double-Affinity Fusion System. Protein Expression and Purification10(3), 309–319.

64. LaVallie ER, DiBlasio EA, Kovacic S, Grant KL, Schendel PF, McCoy JM. (1993) A thioredoxin gene fusion expression system that circumvents inclusion body formation in the E. coli cytoplasm. Biotechnology (N Y). 1993 Feb;11(2):187-93

65. Zhang Y, Olsen DR, Nguyen KB, Olson PS, Rhodes ET, Mascarenhas D. (1998) Expression of eukaryotic proteins in soluble form in Escherichia coli. Protein Expr Purif. 1998 Mar;12(2):159-65.

66. Per-Åke Nygren, Ståhl Stefan, Mathias Uhlén (1994) Engineering proteins to facilitate bioprocessing. Trends in Biotechnology 12(5) 184–188.

67. H. LeVine, 3rd (1993) Thioflavine T interaction with synthetic Alzheimer's disease beta-amyloid peptides: detection of amyloid aggregation in solution. Protein Sci. 19

68. Betts V, Leissring MA, Dolios G, Wang R, Selkoe DJ, Walsh DM (2008) Aggregation and catabolism of disease-associated intra-Abeta mutations: reduced proteolysis of AbetaA21G by neprilysin.Neurobiol.Dis. 2008; 31: 442–45093 March; 2(3): 404–410.

69. Naiki H, Hasegawa K, Yamaguchi I, Nakamura H, Gejyo F, Nakakuki .Apolipoprotein E and antioxidants have different mechanisms of inhibiting Alzheimer's beta-amyloid fibril formation in vitro. Biochemistry 1998; 37: 17882–17889

70. Jan A, Gokce O, Luthi-Carter R, Lashuel HA. The ratio of monomeric to aggregated forms of Abeta40 and Abeta42 is an important determinant of amyloid-beta aggregation, fibrillogenesis, and toxicity.J. Biol. Chem. 2008; 283: 28176–28189.

71. Yoshiike Y, Chui DH, Akagi T, Tanaka N, Takashima A. Specific compositions of amyloid-beta peptides as the determinant of toxic beta-aggregation. J. Biol. Chem. 2003; 278: 23648–23655.

72. Murakami K, Irie K, Morimoto A, Ohigashi H, Shindo M, Nagao M,Shimizu T, Shirasawa T. Synthesis, aggregation, neurotoxicity, and secondary structure of various A beta 1-42 mutants of familial Alzheimer's disease at positions 21-23. Biochem. Biophys. Res.Commun. 2002; 294: 5–10.

73. Shahnawaz M, Thapa A, Park IS (2007) Stable activity of a deubiquitylating enzyme (Usp2-cc) in the presence of high concentrations of urea and its application to purify aggregation-prone peptides. Biochem Biophys Res Commun. 3;359(3):801-5.

74. T.P. Hopp, K.S. Prickett et al. (1988) A short polypeptide marker sequence useful for recombinant protein identification and purification. Nature Biotechnology 6:1204–1210

75. A. Einhauer and A. Jungbaeur (2001) The FLAG™ peptide, a versatile fusion tag for the purification of recombinant proteins. J. Biochem. Biophys. Methods 49:455-65

76. J. Field, J. Nikawa, D. Broek, B. MacDonald, L. Rodgers, I.A. Wilson, R. A. Lerner, and M. Wigler (1988) Purification of a RAS-responsive adenylyl cyclase complex from Saccharomyces cerevisiae by use of an epitope addition method. Mol Cell Biol. 8:2159-65

77. Susan Elmore. (2007) Apoptosis: A Review of Programmed Cell Death.35 (4) 495-516.

78. Ndung'u M, Härtig W, Wegner F, Mwenda JM, Low RW, Akinyemi RO, Kalaria RN. (2012) Cerebral amyloid β(42) deposits and microvascular pathology in ageing baboons. Neuropathol Appl Neurobiol. 2012 38(5):487-99.

79. Pasquale Picone, Rita Carrotta, Giovanna Montana, Maria Rita Nobile, Pier Luigi San Biagio, and Marta Di Carlo (2009) Aβ Oligomers and Fibrillar Aggregates Induce Different Apoptotic Pathways in LAN5 Neuroblastoma Cell Cultures. Biophys J. 2009 20; 96(10): 4200–4211

80. Wogulis M, Wright S, Cunningham D, Chilcote T, Powell K, Rydel RE. (2005) Nucleation-dependent polymerization is an

essential component of amyloid-mediated neuronal cell death. J Neurosci. 2005 Feb 2;25(5):1071-80.

81. Clawson GA, Bui V, Xin P, Wang N, Pan W. (2008) Intracellular localization of the tumor suppressor HtrA1/Prss11 and its association with HPV16 E6 and E7 proteins. J Cell Biochem. 2008 Sep 1;105(1):81-8.

82. Chetan Dhamne, David A. Drubin,Kimberly Duncan, M. Judith Tevethia,Gary A. Clawson (2006) The Chloromethyketone protease inhibitor $AAPF_{CMK}$ also target ATP-dependent Helicase and SAP-Domain proteins.journal of cellular biochemistry 100:716-726.

83. Sandrine Ruchaud, Nadia Korfali, Pascal Villa, Timothy J. Kottke,3 Colin Dingwall,Scott H. Kaufmann, and William C. Earnshaw (2002) Caspase-6 gene disruption reveals a requirement for lamin A cleavage in apoptotic chromatin condensation. EMBO J 21(8): 1967–1977.

84. Andersson M, Sjöstrand J, Petersen A, Honarvar AK, Karlsson JO. (2000) Caspase and proteasome activity during staurosporin-induced apoptosis in lens epithelial cells. Invest Ophthalmol Vis Sci. 2000 41(9):2623-32.

85. Dong Zhang, Paul J. Beresford, Arnold H. Greenberg, and Judy Lieberman. (2001) Granzymes A and B directly cleave lamins and disrupt the nuclear lamina during granule-mediated cytolysis. 98(10) 5746-5751.

86. David J. McConkey (1996) Calcium-dependent, Interleukin 1b-converting Enzyme

Inhibitor-insensitive Degradation of Lamin B1 and DNA Fragmentation in Isolated Thymocyte Nuclei. Journal of biological chemistry271 (37) 22398–22406.

87. Jenny CY Ho, Ting Zhou, Wing-Hon Lai, Yinghua Huang, Yau-Chi Chan, Xingyan Li, Navy LY Wong, Yanhua Li, Ka-Wing Au, Dongsheng Guo, Jianyong Xu, Chung-Wah Siu, Duanqing Pei, Hung-Fat Tse, and Miguel Angel Esteban. (2011) Generation of induced pluripotent stem cell lines from 3 distinct laminopathies bearing heterogeneous mutations in lamin A/C. 3(4)

88. Veronika Butin-Israeli, Orly Ben-nun-Shaul, Idit Kopatz, Stephen A. Adam, Takeshi Shimi, Robert D Goldman and Ariella Oppenheim (2011) Simian virus 40 induces lamin A/C

fluctuations and nuclear envelope deformation during cell entry. 2(4) 320-330.

89. Kuei-Hua Chang,a Parminder Singh Multani,a Kai-Hui Sun,a Fabien Vincent,a Yolanda de Pablo,a Soumitra Ghosh,a Ritika Gupta,a Hyun-Pil Lee,b Hyoung-gon Lee,b Mark A. Smith,b and Kavita Shaha, (2011) Nuclear envelope dispersion triggered by deregulated Cdk5 precedes neuronal death. Mol Biol Cell. 2011 May 1; 22(9): 1452–1462.

90. B. Buendia, A. Santa-Maria and J. C. Courvalin (1999) Caspase-dependent proteolysis of integral and peripheral proteins of nuclear membranes and nuclear pore complex proteins during apoptosis. Journal of Cell Science 112, 1743-1753.

91. J.W. Olney, D.F. Wozniak,V. Jevtovic-Todorovic, Chrysanthy Ikonomidou (2001). Glutamate signaling and fetal glutmate syndrome. Developmental Disabilities Research Reviews 7(4) 267-275.

VII. ACKNOWLEDGEMENTS

Foremost, I would like to record my gratitude to my supervisor Prof. Il-Seon Park for his supervision, advice, and guidance from the early stage of this research and most important giving me extraordinary experiences throughout the work. I would like to extend my sincere gratitude to Prof. Song Yub Shin, Prof. Kun Ho Lee, Prof. Takbum Ohn and Prof. Jung Hee Lee for their encouragement and support in various ways.

I gratefully thank to my friends Dev, Bijoy, Rajesh, Palani, Hari, aravind and kamal for their immense support during my work. I wish to thank my colleagues Imam, Sharoar, Dr. Jung Eun, Jung-Woo for their countless help which made my life easy in Korea. All the members of Molecular and Cell biology, Peptide Biochemistry, Peptide engineering and Korea DNA repair Laboratory get warmest thanks giving me the possibility of sharing their facilities.

Finally, I would like to thank and dedicate my thesis to My parents, My Brother, My wife and daughter for their support and encouragement throughout my academic career.